Article

Functionally Selective Dopamine D2/D3 Receptor Agonists Comprising an Enyne Moiety

Christine Hiller, Ralf C. Kling, Frank W Heinemann, Karsten Meyer, Harald Hübner, and Peter Gmeiner

J. Med. Chem., **Just Accepted Manuscript** • DOI: 10.1021/jm400520c • Publication Date (Web): 03 Jun 2013

Functionally Selective Dopamine D_2/D_3 Receptor Agonists Comprising an Enyne Moiety

*Christine Hiller,[1] Ralf C. Kling,[1] Frank W. Heinemann,[2] Karsten Meyer,[2] Harald Hübner,[1] Peter Gmeiner[1]**

[1]Department of Chemistry and Pharmacy, Medicinal Chemistry, Emil Fischer Center, Friedrich Alexander University, Schuhstraße 19, 91052 Erlangen, Germany.

[2]Department of Chemistry and Pharmacy, Inorganic Chemistry, Friedrich Alexander University, Egerlandstraße 1, 91058 Erlangen, Germany.

RECEIVED DATE (to be automatically inserted)

TITLE RUNNING HEAD: Functionally Selective Enynes

KEYWORDS: GPCR, dopamine receptor, functional selectivity, ligand bias, G protein, β-arrestin

Abstract:

Dopaminergics of type **1** and **2** incorporating a conjugated enyne as an atypical catechol-simulating moiety were synthesized in enantiomerically pure form and investigated for their metabolic stability. Radioligand binding studies indicated high affinity to D_2-like receptors. The test compounds were evaluated for their ability to differentially activate distinct signaling pathways. Measurement of D_{2L}- and D_{2S}-mediated [^{35}S]GTPγS incorporation in the presence of co-expressed $G\alpha_o$ and $G\alpha_i$ subunits showed significantly biased receptor activation for several test compounds. Thus, the 2-azaindolyl carboxamide **(*S*)-2a** exhibited substantial functional selectivity for D_{2S}-promoted G_o activation over G_i coupling. The most significant bias was determined for the triazolylalkoxy-substituted benzamide **(*S*)-2c** that displayed higher potency for G_o activation than for G_i coupling at the D_{2L} subtype. Functional selectivity for β-arrestin recruitment over G_i activation was observed for the biphenylcarboxamide **(*R*)-1** and the 2-benzothiophenyl carboxamide **(*S*)-2d** whereas the 2-substituted azaindole **(*S*)-2a** preferred β-arrestin recruitment compared to G_o coupling.

Introduction

Agonist-induced coupling of one type of receptor to multiple signaling pathways is a general property of G protein-coupled receptors (GPCRs).[1] Functional selectivity explains the capacity of a ligand to preferentially activate coupling of a GPCR with a subset of signal transducers. Thus, ligand-GPCR interactions can promote an individual pattern of G protein-dependent and G protein-independent signaling. Employing the angiotensin II receptor as a model system, pioneering work of R. Lefkowitz et al. showed that G protein- and β-arrestin-mediated pathways can be pharmacologically modulated independently with functionally selective ligands.[2, 3] Excellent recent studies provided structural insights into the phenomenon of biased signaling.[4, 5] Ligand-induced bias between G protein coupling and β-arrestin recruitment was also reported for the dopaminergic drug aripiprazole and structurally related analogs.[6-8]

Dopamine D_2 and D_3 receptors are known as valuable targets for the treatment of neurological and psychiatric disorders involving Parkinson's disease, dyskinesia, restless legs syndrome and schizophrenia.[9-13] Whereas highly selective coupling to $G_{\alpha o}$ was demonstrated for the D_3 subtype, promiscuity in G protein coupling was shown for D_2 existing in the splice variants D_{2long} (D_{2L}) and D_{2short} (D_{2S}).[14, 15] Besides agonist-mediated inhibition of calcium channels, G_o signaling activates other intracellular effectors like potassium channels and MAP-kinases but does not affect intracellular cAMP levels.[16, 17] In contrast, coupling to G_i subtypes led to inhibition of adenylyl cyclase and ERK activation.[18-21] Co-expression of D_2 with the G proteins G_o and G_i indicated the formation of ligand – specific ternary complexes.[15, 22] Because novel types of agonists will have the potential to control dopamine-mediated pharmacology in a unique way, our very recent efforts focused on the identification and optimization of functionally selective dopaminergics. Starting from phenylpiperazine derivatives, which are known as

privileged structures for dopamine receptor antagonists,[23] we developed the functionally biased dopamine D_2 receptor ligand *N*-[3-[4-(2,3-dihydrobenzofuran-7-yl)piperazin-1-yl]propyl]pyrazolo[1,5-*a*]pyridine-3-carboxamide (FAUC350), which behaves as an antagonist in the inhibition of cAMP accumulation and as a partial agonist in the stimulation of ERK1/2 phosphorylation.[24] As a complement to these studies, we intended to investigate a family of compounds with a dopamine agonist pharmacophore for their ability to differentiate between G_o- and G_i-mediated signaling. Our initial investigations using agonists with classical catechol-simulating functional groups indicated only a weak ability to differentiate between G_o- and G_i-induced D_2 receptor activation in a GTPγS assay (see, Supporting Information). Thus, we intended to build our work on atypical bioisosteres such as conjugated enynes.[25-29] Because we were concerned that diasteric G_o/G_i preferences of enantiomers might make it difficult to interpret our data correctly, an chirospecific synthetic approach was chosen. In this study, we present chemical synthesis and *in vitro* biological evaluations of dopaminergic enynes of type **1** and **2** (Figure 1) in enantiomerically pure form.

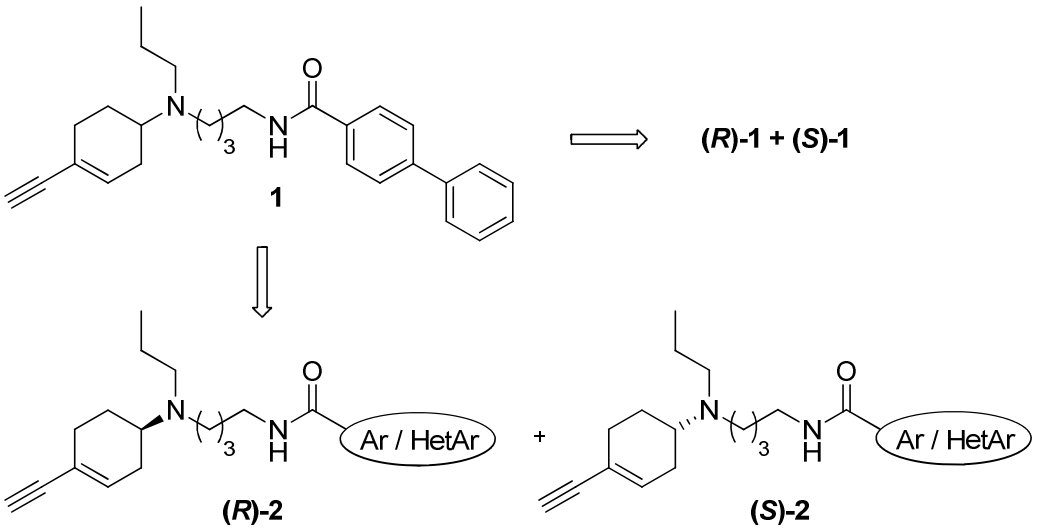

Figure 1. Chiral resolution and structural modifications leading to enantiomerically pure target compounds of type **1** and **2**.

Results and Discussion

Synthesis. To investigate enantiospecific ligand-receptor interactions of dopaminergic alkynylcyclohexenylamines, a collection of derivatives was synthesized in enantiomerically pure form by functionalization of the monopropylamines **(*R*)-6** and **(*S*)-6** (Scheme 1) that contain an asymmetric carbon in the cyclohexene ring as a source of chirality. Since our previously described reaction sequence for the preparation of racemic alkynylcyclohexenylamines[29] was not suitable to access secondary amines of type **6**, an alternative pathway was elaborated. Our synthesis started from the 1,4-cyclohexanedione monoethylene acetal, which was converted to the tertiary alcohol **3** by *Grignard* reaction. Subsequent hydrolysis of the acetal protecting group and reductive amination of the resulting ketone **4** with propylamine and sodium triacetoxyborohydride afforded the aminoalcohol **5**, which was dehydrated using a reaction mixture of PPh_3, I_2 and imidazole to give the racemic secondary amine **6** in excellent overall yield (52%).[30, 31] To obtain the pure enantiomers **(*R*)-6** and **(*S*)-6**, chiral resolution was accomplished by preparative HPLC employing a polysaccharide-based column (Chiralpak® AS-H) resulting in ee values greater 99%. For an unambiguous assignment of the absolute configuration, we intended to obtain a high resolution crystal structure. Because attempts to grow crystals of the pure enantiomers suitable for X-ray analysis failed, derivatization by acylation with 3,5-dinitrobenzoyl chloride was conducted to yield the readily crystallizable amide **(*S*)-7** from the homochiral secondary amine.

Scheme 1.[a]

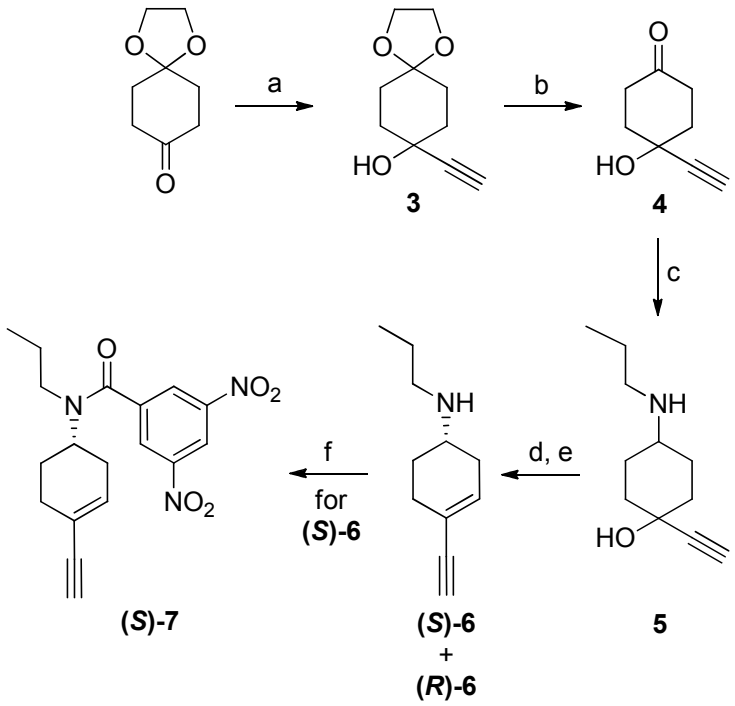

[a] Reagents and conditions: (a) ethynylmagnesium bromide, THF, 0 °C to rt, 2 h (90%); (b) 80% HCOOH, $CuSO_4$, rt, 16 h (79%); (c) propylamine, $NaBH(OAc)_3$, AcOH, DCM, 0 °C to rt, 4 h (80%); (d) PPh_3, I_2, imidazole, DCM, 16 h (94%); (e) chiral resolution by preparative HPLC using Chiralpak AS-H column; (f) 3,5-dinitrobenzoyl chloride, Et_3N, DCM, 0 °C, 4 h (86%).

X-ray diffraction analysis of the benzamide **(*S*)-7** (Figure 2) revealed the presence of two independent molecules in the asymmetric unit. Both molecules clearly exhibit (*S*)-configuration at the stereogenic center but different conformation of the dinitrophenyl moiety (*cf.* Figs. S1 and S2, supporting information). The crystal structure further indicated a half-chair conformation of the cyclohexene ring with an equatorially positioned carboxamide group for both of the independent molecules.

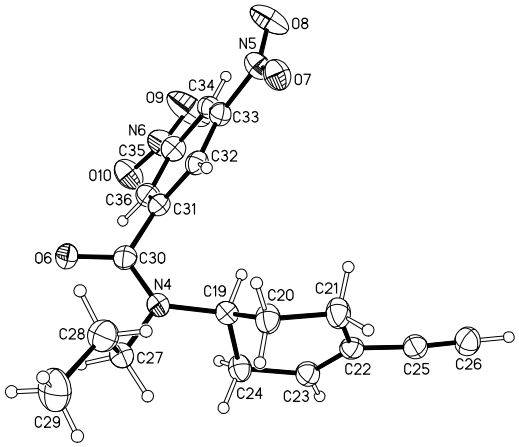

Figure 2. Thermal ellipsoid representation of the molecular structure of one out of two independent molecules of the 3,5-dinitrobenzamide **(*S*)-7**, determined by X-ray crystal structure analysis (50% probability ellipsoids, hydrogen atoms drawn as spheres of arbitrary size).

The test compounds of type **1** and **2** were synthesized by reductive alkylation of the enantiopure intermediates **(*R*)-6** and **(*S*)-6** with the *N*-(4-hydroxybutyl)aryl carboxamides **8**–**13** (Scheme 2). In detail, the starting compounds **8**–**13** were prepared by *N*-acylation of 4-aminobutanol with commercially available biphenyl-4-carbonyl chloride or by CDI-mediated amidation of 4-aminobutanol with pyrazolo[1,5-*a*]pyridinyl, benzo[*b*]thiophenyl and ferrocenyl carboxylic acids as well as the recently described 4-[3-(1-butyl-1*H*-1,2,3-triazol-4-yl)propoxy]-3-methoxybenzoic acid.[32] Subsequent oxidation of the hydroxyl group using pyridine sulfur trioxide furnished the corresponding aldehydes,[33] which were used without further purification to reductively alkylate the secondary amines **(*R*)-** and **(*S*)-6** in presence of sodium triacetoxyborohydride to afford the test compounds **(*R*)-/(*S*)-1** and **(*R*)-/(*S*)-2a**-**2e**.

Scheme 2.[a]

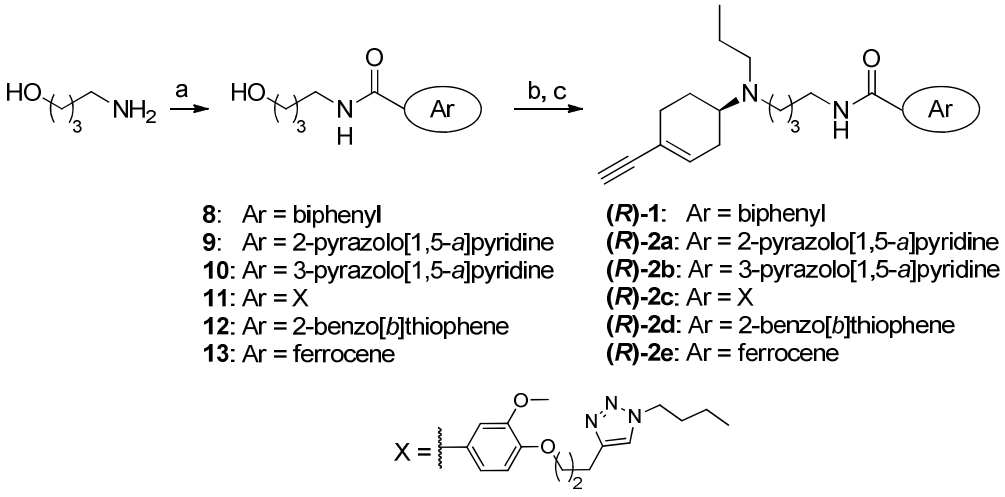

[a] Reagents and conditions: (a) aqueous NaOH, biphenyl-4-carbonyl chloride, DCM, 0 °C to rt, 1 h or Ar-COOH, CDI, DMF, 50 °, 2 h, after cooling to rt: addition of 4-aminobutanol, 2 h (58-94%); (b) pyridine sulfur trioxide, Et_3N, DCM/DMSO, 0 °C to rt, 1 h; (c) **(*R*)**- or **(*S*)-6**, $NaBH(OAc)_3$, DCM, rt, 3-5 h (36-71%).

Biological Investigations.

Studies on Metabolic Stability.

Dopamine receptor agonists including ropinirole (4-[2-(dipropylamino)ethyl]-1,3-dihydro-2*H*-indol-2-one) and rotigotine ((*S*)-2-(*N*-propyl-*N*-2-thienylethylamino)-5-hydroxytetralin), which have been developed for the treatment of Parkinson's disease, are known to be extensively metabolized.[34, 35] Due to a substantial first-pass effect, rotigotine displays an oral bioavailability of only 0.5%.[36] Metabolism studies using isolated rat liver perfusion technique detected 15 different metabolites, whereas *N*-dealkylation and hydroxylation were identified as major metabolic pathways.[37] Hence, we were intrigued by the question whether our newly developed enyne derivatives display stability against oxidative biotransformation reactions. Due to its

substantial metabolism, rotigotine was chosen as a positive control to validate the assay. Interestingly, *in vitro* metabolism studies using rat liver microsomes revealed superior stability for the alkynylcyclohexenylamine **1** (used in racemic form) when compared to the reference agent rotigotine. After 15 min, only 41.8% of rotigotine remained unchanged, whereas the enzymatic biotransformation of the enyne bearing dopaminergic **1** proceeded significantly slower (Figure 3). More than 70% of the starting material could still be detected after an incubation time of 60 min. Thus, the metabolism profile of our alkynylcyclohexenylamines is comparable to the approved drug pramipexole, which is known to be cleared largely unchanged.[38]

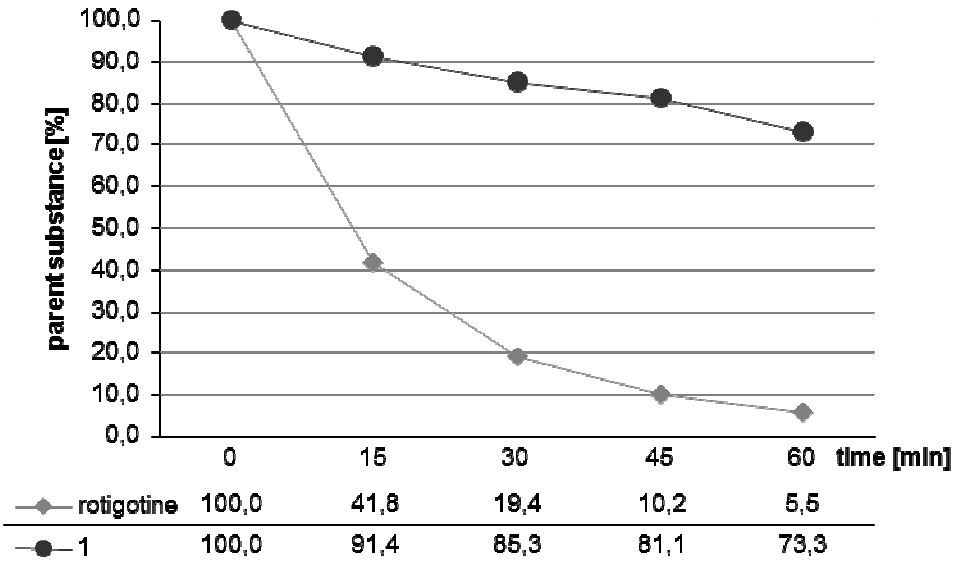

Figure 3. Oxidative metabolism profile of rotigotine and the biphenylcarboxamide **1**.Results as mean percentages of non-metabolized parent compound. Incubations were performed using 0.05 mg/mL of rotigotine or **1**, pooled rat liver microsomes (1.0 mg/mL) in the presence of 1 mM NADPH at 37 °C for 60 min. Aliquots were drawn after predetermined time intervals of 0, 15, 30, 45 and 60 min. All incubations were performed in duplicate.

LC/MS analysis of the slowly formed metabolites revealed *N*-depropylation as major metabolic pathway to give the derivative **14** (Figure 4).[34, 37, 39, 40] Besides *N*-depropylation, the biphenylcarboxamide **1** showed additional enzyme catalyzed cleavage of the ethynylcyclohexene

residue resulting in the secondary amine **15** and oxidation of the ethynyl substituent to yield the carboxylic acid **16.**

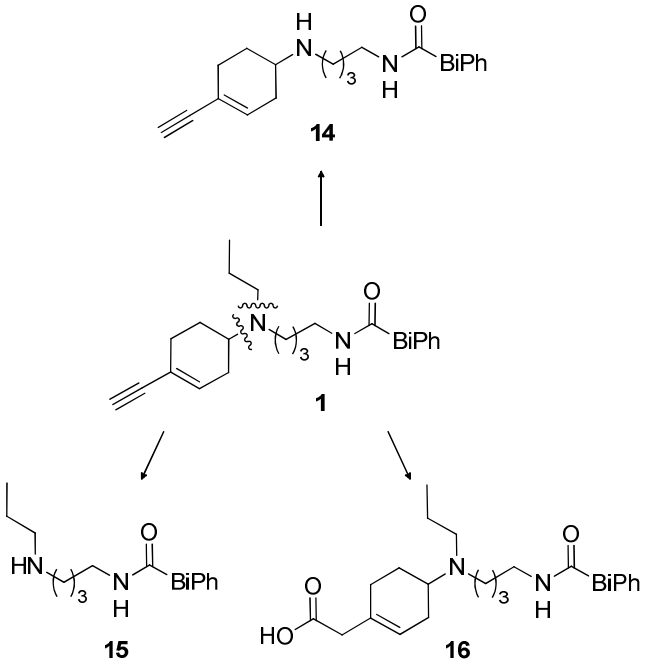

Figure 4. Biotransformation pathway of the biphenylcarboxamide **1**.

Ligand Binding Experiments. To evaluate receptor binding of the enantiopure test compounds of type **1** and **2**, radioligand displacement assays were conducted. The binding affinity and selectivity profiles of the target compounds were compared with those of the reference agent quinpirole (Table 1).[41] Binding data were generated by measuring the ability of the test compounds to compete with [^{3}H]spiperone for the cloned human dopamine receptor subtypes D_{2L}, D_{2S}, D_3, and $D_{4.4}$ stably expressed in Chinese hamster ovary (CHO) cells. D_1 receptor affinities were determined utilizing porcine striatal membranes and the D_1 selective radioligand 7-chloro-3-methyl-1-phenyl-1,2,4,5-tetrahydro-3-benzazepin-8-ol ([^{3}H]SCH 23390). Because the preferred binding of D_2 agonists to the ternary complex is known to result in significantly

different values for $K_{i\ high}$ and $K_{i\ low}$, the high affinity binding site of D_{2L}, selectively labeled by the D_2 agonist 2-dipropylamino-7-hydroxy-1,2,3,4-tetrahydronaphthalene ([^{3}H]7-OH-DPAT), was also subjected to ligand competition experiments. In fact, all test compounds of type **1** and **2** showed high binding affinity resulting in K_i values between 0.53 and 5.5 nM. Eudysmic ratios for the enantiomers were close to one except for the triazolyl substituted dialkoxybenzamide **2c** that gave a factor of approximately 8 when the (*S*)-enantiomer showed higher affinity. Our subsequent investigations were directed to comprehensive evaluation of the enantiomers of **(*R*)-1** and **(*S*)-1**, which we described in racemic form (*rac*-**1**, FAUC 460) earlier, involving the above mentioned monoaminergic GPCRs.[29] The data indicate an agreement of the binding profiles and only minor stereospecific differences between the optical antipodes. Both enantiomers displayed substantial D_3 affinity and selectivity. Formal exchange of the biphenylcarboxamide moiety by a pyrazolo[1,5-*a*]pyridine-3-ylcarboxamide unit led to more balanced binding profiles for the heterocyclic bioisosteres **(*R*)-2b** and **(*S*)-2b**. Thus, K_i values between 7.1 and 22 nM were determined for the D2-like subtypes D_{2L}, D_{2S}, D_3 and $D_{4.4}$ indicating significant receptor recognition in low concentration. While the 2-substituted isomers **(*R*)-2a** and **(*S*)-2a** and its benzothiophene analogs **(*R*)-2d** and **(*S*)-2d** displayed D_3 preference, the ferrocenylcarboxamides **(*R*)-2e** and **(*S*)-2e** revealed subnanomolar affinity for the two subtypes D_3 and $D_{4.4}$. The binding pattern of the dialkoxybenzamides **(*R*)-2c** and **(*S*)-2c** indicated a balanced binding to D_{2L}, D_{2S} and D_3 with K_i values between 1.0 and 8.0 nM. All test compounds of type **1** and **2** showed only moderate to poor affinity to the porcine receptors of the adrenergic, dopaminergic and serotonergic subtypes α_1, D_1 and 5-HT_2, respectively. However, K_i-values in the nanomolar range were observed for 5-HT_{1A}, when the ferrocene derivatives **(*R*)-2e** and **(*S*)-2e** gave even

single-digit values. Worthy of note is also the poor ability of enantiomeric test compounds to differentially bind the investigated receptors.

Table 1. Receptor Binding Data of (*R*)-/(*S*)-**1** and (*R*)-/(*S*)-**2a**–**2e** Compared to the Reference Compound Quinpirole Utilizing Human D_{2L}, D_{2S}, D_3 and $D_{4.4}$ Receptors as well as Porcine D_1, 5-HT_{1A}, 5-HT_2 and α_1 Receptors.

compd	K_i values [nM ± SEM][a]								
	[³H]SCH23390	[³H]7-OH-DPAT	[³H]spiperone				[³H]WAY100635	[³H]ketanserin	[³H]prazosin
	pD_1	D_{2L}	D_{2L}	D_{2S}	D_3	$D_{4.4}$	p5-HT_{1A}	p5-HT_2	pα_1
quinpirole	87000 ± 6000	18 ± 3.2	260 ± 38	70 ± 18	15 ± 3.7	8.5 ± 1.4	6300 ± 1100	25000 ± 9200	55000 ± 6200
(R)-**1**	300 ± 64[b]	0.60 ± 0.27	11 ± 2.1	18 ± 3.1	0.12 ± 0.035	5.8 ± 1.1	140 ± 28[b]	190 ± 35[b]	220 ± 14[b]
(S)-**1**	190 ± 57	1.2 ± 0.82	14 ± 2.4	21 ± 5.5	0.17 ± 0.036	11 ± 3.2	280 ± 42[b]	210 ± 35[b]	130 ± 14[b]
(R)-**2a**	25000 ± 2800	5.5 ± 1.5[b]	63 ± 13	230 ± 68	3.2 ± 0.33	37 ± 3.5	33 ± 10	18000 ± 9200[b]	1100 ± 520[b]
(S)-**2a**	45000 ± 6400[b]	3.9 ± 1.0	66 ± 18	280 ± 91	10 ± 1.5	110 ± 14	150 ± 35	35000 ± 8400[b]	2900 ± 1900[b]
(R)-**2b**	36000 ± 3500[b]	0.55 ± 0.13	7.1 ± 3.8	9.3 ± 1.1	8.6 ± 0.66	14 ± 3.7	23 ± 2.1	16000 ± 2100	730 ± 290
(S)-**2b**	33000 ± 4900[b]	1.1 ± 0.33	7.8 ± 1.8	14 ± 2.5	10 ± 1.6	22 ± 6.0	48 ± 17	13000 ± 710[b]	1500 ± 710[b]
(R)-**2c**	18000 ± 6400[b]	4.2 ± 2.4	8.0 ± 0.91	8.8 ± 2.2	4.3 ± 1.7	59 ± 18	110 ± 17[b]	28000 ± 13000[b]	1800 ± 350[b]
(S)-**2c**	13000 ± 5100[b]	0.53 ± 0.13	6.0 ± 0.83	3.9 ± 1.6	1.0 ± 0.30	30 ± 8.1	160 ± 42[b]	8500 ± 3500[b]	620 ± 160[b]
(R)-**2d**	5500 ± 70[b]	3.1 ± 1.3	32 ± 4.6	33 ± 9.7	0.24 ± 0.069	5.3 ± 0.91	40 ± 3.5[b]	2100 ± 210[b]	170 ± 57[b]
(S)-**2d**	4700 ± 640[b]	2.0 ± 0.67	22 ± 4.6	16 ± 2.8	0.43 ± 0.17	4.8 ± 1.4	65 ± 25[b]	1300 ± 570[b]	200 ± 21[b]
(R)-**2e**	19000 ± 4300	1.1 ± 0.55	14 ± 3.0	13 ± 2.3	0.63 ± 0.15	0.89 ± 0.17	4.0 ± 1.0	5800 ± 520	1400 ± 230
(S)-**2e**	16000 ± 1600	1.1 ± 0.50	14 ± 3.6	16 ± 3.0	0.34 ± 0.085	0.73 ± 0.13	3.7 ± 1.4	3500 ± 450	280 ± 73

[a] K_i values in nM ± standard error of mean derived from 3-10 experiments each done in triplicate. [b] K_i values ± standard deviation derived from two individual experiments each done in triplicate.

Functional Experiments. Functional selectivity explains the ability of a ligand to preferentially activate coupling of a GPCR with a subset of signal transducers. To investigate the capability of our newly synthesized test compounds to perform balanced or biased receptor activation, the pertussis toxin (PTX) insensitive G protein subunits $G\alpha_o$ or $G\alpha_i$[42] were co-transfected with the dopamine receptor isoforms D_{2L} and D_{2S}. We intended to measure D_{2L} and D_{2S} receptor-mediated incorporation of [^{35}S]GTPγS when our initial investigations were focused on the characterization of the reference agent quinpirole (Figure 5).

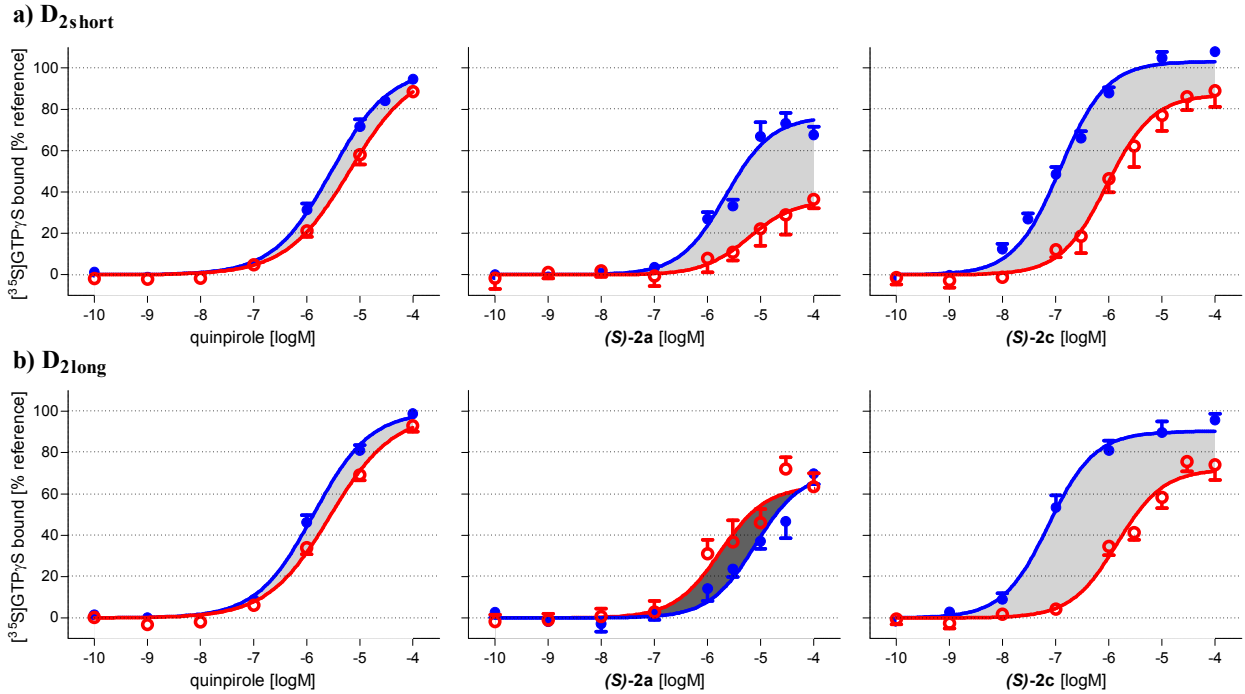

Figure 5. Dose-response curves of the agonist stimulated [^{35}S]GTPγS binding at the dopamine receptor subtypes D_{2S}(a) and D_{2L} (b). Membranes from cells transiently transfected with D_{2S} or D_{2L} and the PTX-insensitive G proteins $G\alpha_{o1}$ or $G\alpha_{i2}$ were stimulated with ***(S)*-2a**, ***(S)*-2c** or the reference agonist quinpirole. The difference between the areas under the curves (AUCs) for the graphs derived from the D_2+$G\alpha_{o1}$ (blue) system and the ones displaying D_2+$G\alpha_{i2}$ (red) is highlighted in light grey and indicate a selectivity of $G\alpha_{o1}$ over $G\alpha_{i2}$. The difference of AUCs for ***(S)*-2a** at D_{2L} (dark grey) displays a selectivity of $G\alpha_{i2}$ over $G\alpha_{o1}$.

The dose-response curves for D_{2S} receptors co-transfected either with the G protein subunit $G\alpha_o$ or $G\alpha_i$ showed very similar potency and ligand efficacy when receptor activation was promoted by quinpirole. For co-transfections of D_{2L} with $G\alpha_o$ or $G\alpha_i$, the same observation was made. In both cases, the (grey) area indicating the difference between the areas under the curve (AUC) of the G_o-mediated response (blue) and the G_i-mediated activation (red) displays only a minor bias for one of the coupling opportunities, namely for G_o.

In contrast, the ability of the test compounds to differentiate between G_o- and G_i-mediated receptor activation was considerably more pronounced. Thus, the large area between the dose-response curves of the 2-azaindolyl substituted test compound ***(S)*-2a** shows that the ligand efficacy for D_{2S} receptors co-transfected with $G\alpha_o$ is substantially higher than for the D_{2S}-$G\alpha_i$ system. Interestingly, an inverse behavior was observed for ***(S)*-2a**-promoted activation of D_{2L} when the G_i-induced response was superior. Besides maximal ligand efficacy of the test compounds (E_{max}), functional selectivity can be also induced by different potencies. An impressive example is the triazolylalkyoxyphenyl substituted test compound ***(S)*-2c** causing different AUCs by the ability of the test compound to promote $G\alpha_o$ activation at much lower concentrations than $G\alpha_i$ coupling. This property could be observed for both test systems expressing D_{2L} and D_{2S}.

Because we thought that comparison of the individual test compounds' ΔAUCs with those of our traditional reference agent quinpirole was a good measure for functional selectivity, we calculated their relationships by determining the difference of ΔAUCs for the test compound and the reference agent and dividing the result by the ΔAUC value of the reference agent. Thus, a value of 0 means that the compound has a profile that is identical to quinpirole, positive functional selectivity indices (FSIs) indicate a bias for G_o and negative FSI values implicate G_i

selectivity. Table 2 shows that all test compounds displayed substantial bias for D_{2S}-promoted G_o activation with functional selectivity indices between 1.23 and 3.85. Enantiospecificity of the ligand-promoted signaling bias was low for all enyne derivatives that we investigated, indicating that the overall shape and the ligand recognition of both enantiomers at the D_{2S} binding site not only results in a similar ligand affinity but also in a comparable stabilization of individual ternary complexes.

Table 2. Intrinsic Activities of **(*R*)-/(*S*)-1** and **(*R*)-/(*S*)-2a-2e** Determined at the Dopamine Receptor Subtypes D_{2L} and D_{2S} by Measuring the Binding of [^{35}S]GTPγS and the Recruitment of β-Arrestin-2 After Stimulation of the D_{2S} Receptor.

compd	D_{2L}			D_{2S}			
	[^{35}S]GTPγS binding			[^{35}S]GTPγS binding			β-arrestin[a]
	$G\alpha_{i2}$ (E_{max})[b]	$G\alpha_{o1}$ (E_{max})[b]	FSI[c]	$G\alpha_{i2}$ (E_{max})[b]	$G\alpha_{o1}$ (E_{max})[b]	FSI[c]	E_{max}[d]
(R)-**1**	49	44	-0.41	45[e]	62	2.65	79 ± 6.7
(S)-**1**	23	53	2.85	78[e]	62	1.73	62 ± 7.9
(R)-**2a**	53[e]	38	0.93	50	67	2.12	68 ± 4.6
(S)-**2a**	62	71	-2.37	77	37	2.08	62 ± 4.9
(R)-**2b**	24	45	1.67	53	63	1.23	76 ± 4.0
(S)-**2b**	66[e]	53	1.26	59	78	2.85	73 ± 6.1
(R)-**2c**	57	75	1.78	68	94	3.38	100 ± 6.5
(S)-**2c**	72	90	4.30	87	103	3.85	99 ± 3.6
(R)-**2d**	37	60	-0.07	31	60	1.69	51 ± 5.6
(S)-**2d**	31	40	-0.15	41	69	1.85	57 ± 4.8
(R)-**2e**	71	51	-0.33	71	81	1.69	89 ± 3.7
(S)-**2e**	103[e]	57	0.26	85	87	1.73	96 ± 4.6

[a] D_{2S}-mediated recruitment of β-arrestin-2 determined with the PathHunter® Assay; [b] maximum stimulation of [^{35}S]GTPγS binding derived from saturation concentrations of the test compounds from the pooled curve of three to six individual experiments each done in triplicate; E_{max} in [%] relative to the effect of the reference agonist quinpirole; [c] functional selectivity index (FSI) calculated using the formula (ΔAUC[test($G\alpha_o$-$G\alpha_i$)]-ΔAUC[ref($G\alpha_o$-

$G\alpha_i$)])/ΔAUC[ref($G\alpha_o$-$G\alpha_i$)]; [d] D_{2S} mediated recruitment of β-arrestin in [% ± SEM] analyzed from 6-8 individual experiments each done in triplicate at a concentration of 10^{-5} M relative to the effect of the reference agonist quinpirole; [e] no gain of saturation in [^{35}S]GTPγS binding up to a concentration of 10^{-4} M, maximum effect determined at 10^{-4} M.

For D_{2L}-promoted activation the variability of the functional selectivity indices was much higher varying between -2.37 for the *(S)*-enantiomer of the 2-substituted azaindole **2a** and 4.30 for the triazolylalkoxy-substituted benzamide ***(S)*-2c**. For D_{2L}, functional selectivity turned out to be strongly dependent on the nature of the carboxamide substituent. Only six of the twelve compounds investigated showed FSIs higher than 1 or below -1. It is interesting of note that the 2-substituted azaindole carboxamide **2a** showed significant enantiospecific coupling bias when the *(R)*-isomer displayed selectivity for G_o coupling and the *(S)*-enantiomer gave a higher potency for G_i-promoted activation. In contrast, preferential G_o activation of the biphenyl carboxamide **1** depends on the *(S)*-configuration at the stereogenic center.

Receptor mediated recruitment of β-arrestin-2 was determined utilizing assay technology that is based on the complementation of enzyme fragments of β-galactosidase (β-gal). For this purpose, HEK-293 cells stably expressing a fusion protein of β-arrestin and the N-terminal fragment of β-gal were transiently transfected with D_{2S} fused to the C-terminal fragment of the enzyme. After stimulation of the cells with the appropriate agonists, β-arrestin recruitment could be monitored by measuring the occurring chemiluminescence. To investigate whether the synthesized enynes show a G protein-independent signaling, we determined the D_{2S}-mediated β-arrestin recruitment at 10 μM for **(*R*)-/(*S*)-1** and **(*R*)-/(*S*)-2a-2e** in comparison to the effect of quinpirole. Significant β-arrestin recruitment of 50 to 100% relative to the reference compound quinpirole was determined for the test compounds of type **1** and **2**. Highest E_{max} values were observed for the triazolylalkoxy-substituted benzamide **(*R*)/*(S)*-2c.** Whereas in most cases ligand specific β-

arrestin recruitment was similar to the intensity of G protein activation, the biphenyl carboxamide **(*R*)-1** and the 2-benzothiophenyl carboxamide **(*R*)-2d** showed substantial bias for β-arrestin recruitment over G_i activation (G_i : β-arrestin = 57-60%). In contrast, the 2-substituted azaindole **(*S*)-2a** preferred β-arrestin recruitment compared to G_o coupling (G_o : β-arrestin = 57-60%).

Ligand receptor interactions

To explore the relationship between functional selectivity and the individual contacts that are formed between the ligands and the receptor binding site, docking studies were performed. Thus, we established a homology model of the D_2 receptor based on the crystal structure of the D_3 receptor[43] and compared the binding modes of our reference compound quinpirole with the functionally selective test compound **(*S*)-2c** (Figure 6). Quinpirole and the enyne moiety of **(*S*)-2c** occupy the orthosteric binding pocket formed by residues of transmembrane helices (TMs) 3, 5, 6, 7 and extracellular loop 2 (EL2) showing hydrophobic interactions to V3.33, C3.36, F5.38, W6.48, F6.51, F6.52, H6.55 and F7.38 as well as I183 and I184 of EL2 (Figure 6, grey sticks). The propyl groups of both ligands are enclosed in a pocket comprising residues D3.32, W6.48, F6.52, Y7.35, F7.38, T7.39 and Y7.43. The ligands exhibit the canonical salt bridge between their positively charged nitrogen and the carboxylate of D3.32. In contrast to quinpirole, the functionally selective agonist **(*S*)-2c** exhibits additional interactions to residues that are located at an extended binding pocket closer to the extracellular surface of the receptor and spanned by TM 2, 3, 5, 6, 7 and EL2 (Figure 6, blue sticks). The amide and the methoxyphenyl moieties of **(*S*)-2c** are surrounded by residues V2.61, L2.64, E2.65, C182 (EL2), F3.28, V3.29, Y7.35, S7.36 and T7.39. This cavity has been shown to be connected to conformational changes upon activation

and to be involved in functionally selective signaling.[44] The triazole moiety of **(*S*)-2c** bearing the terminal butyl chain points into the direction of TM 5, thereby forming a lid over the extracellular entrance of D_2 and establishing interactions to residues I183 and A185 of EL2, N6.58, I6.59, P7.32 and Y7.35. Recent crystal structures of 5-HT_{1B}[45] and 5-HT_{2B}[5] receptors suggested residues homologous to N6.58 and I6.59 of D_2 to contribute to adjusting a receptor conformation that specifically favors binding of one signal transducer over the other. Within the structure of 5-HT_{2B}, the co-crystallized ligand ergotamine has been shown to behave as a functionally selective agonist inducing β-arrestin signaling to a higher extent than coupling to G proteins and that this effect is more pronounced compared to smaller ligands like lysergic acid diethylamide (LSD) and methylergonovine.[5] As ergotamine connects both, the orthosteric and an extended binding pocket, it is capable of stabilizing a distinct receptor conformation that specifically interferes with G protein binding. Comparable to ergotamine, our functionally selective D_2 agonist **(*S*)-2c** occupies the orthosteric and an extended binding pocket (Figure 6, Supporting Information), which might be the origin for the preference of receptor conformations associated with an atypical signal transducing profile.

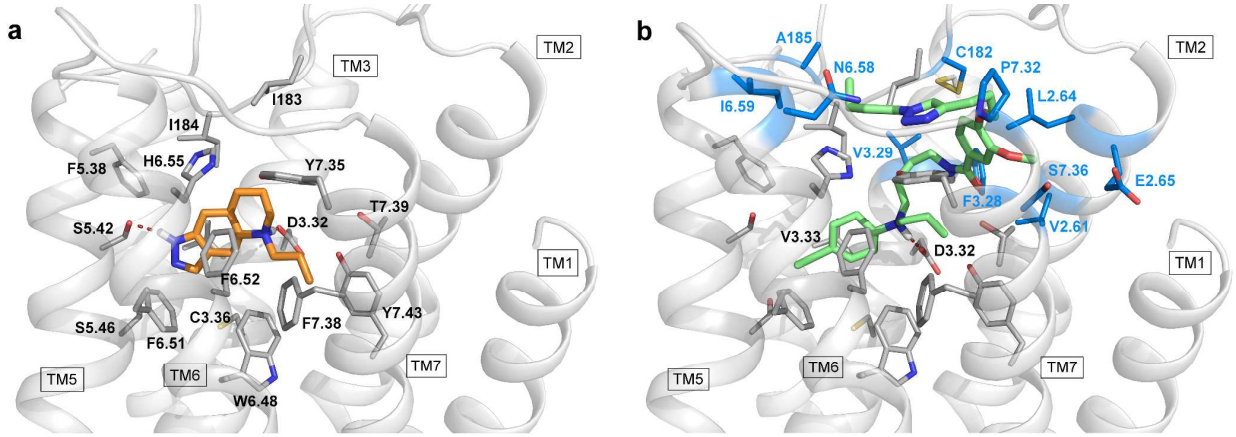

Figure 6. Ligand-receptor interactions for quinpirole (a) and **(*S*)-2c** (b). The backbone of the D_2 model is represented as light grey ribbons, quinpirole and **(*S*)-2c** are shown as orange and green sticks, respectively. Amino acids stabilizing both ligands are visualized as grey sticks, whereas

additional amino acids comprising an extended binding pocket of **(*S*)-2c** are highlighted as blue sticks. The figure was prepared using PyMOL.

Conclusion

Functional selectivity explains the capacity of a ligand to preferentially activate coupling of a GPCR with a subset of signal transducers. Enantiomerically pure dopaminergics of type **1** and **2** incorporating a conjugated enyne as an atypical catechol-simulating moiety were investigated. Metabolism studies revealed the atypical pharmacophores to be stable against oxidative biotransformation reactions. Radioligand binding studies indicated substantial affinity to D_2-like receptors.

The test compounds were studied for their ability to differentially activate distinct signaling pathways. Measurement of D_{2L}- and D_{2S}-mediated [^{35}S]GTPγS incorporation in the presence of coexpressed PTX-insensitive $G\alpha_o$ and $G\alpha_i$ subunits showed significantly biased receptor activation for several test compounds. Compared to the reference agent quinpirole that displayed only a minor bias for G_o coupling the 2-azaindolyl carboxamide **(*S*)-2a** exhibited substantial selectivity for D_{2S}-promoted G_o activation over G_i coupling. The highest functional selectivity was determined for the triazolylalkoxy-substituted benzamide **(*S*)-2c** that displayed higher potency for G_o activation than for G_i coupling at the D_{2L} subtype. Compared to the reference compound quinpirole, significant bias for β-arrestin recruitment over G_i activation was observed for the biphenylcarboxamide **(*R*)-1** and the 2-benzothiophenyl carboxamide **(*R*)-2d**, whereas the 2-substituted azaindole **(*S*)-2a** preferred β-arrestin recruitment compared to G_o coupling. These observations demonstrate the feasibility of differentially activating distinct signaling pathways by biased agonists. Further investigations are needed to determine the consequences of biased agonism *in vivo* and to elucidate structural properties that trigger functional selectivity.

Experimental section

Chemistry. All reactions were carried out under nitrogen atmosphere. Reagents and dry solvents were of commercial quality and were used as purchased. MS were run on a JEOL JMS-GC Mate II spectrometer by EI (70 eV) with solid inlet or a Bruker Esquire 2000 by APC or ES ionization. HR-EIMS was run on a JOEL JMS-GC Mate II using Peak-Matching (M/ΔM > 5000). NMR spectra were obtained on a Bruker Avance 360 or a Bruker Avance 600 spectrometer relative to TMS in the solvents indicated (*J* value in hertz). Melting points were determined with a MEL-TEMP II melting point apparatus (Laboratory Devices, USA) in open capillaries and are given uncorrected. IR spectra were performed on a Jasco FT/IR 410 spectrometer. Purification by flash chromatography was performed using Silica Gel 60; TLC analyses were performed using Merck 60 F254 aluminum sheets and analyzed by UV light, (254 nm), in the presence of iodine or by spraying with ninhydrin reagent. Analytical HPLC was performed on Agilent 1100 HPLC systems employing a VWL detector or on Agilent 1200 HPLC systems using a DAD detector. As column, a ZORBAX ECLIPSE XDB-C8 (4.6 mm x 150 mm, 5 μm) was used. HPLC purity was measured using following binary solvent systems: system A, eluent CH_3OH in 0.1% aqueous formic acid, 10% to 100% CH_3OH in 15 min, 100% for 6 min, flow rate 0.5 mL/min, λ 254 nm or 220 nm; system B, eluent CH_3CN in 0.1% aqueous formic acid, 5% to 80% in 18 min, 80% to 95% in 2 min, 95% for 2 min, flow rate 0.5 mL/min, λ 254 nm or 220 nm. The purity of all test compounds and key intermediates was determined to be > 95%. Preparative HPLC was performed on Agilent 1100 HPLC systems employing a VWL detector.

(*R*)-*N*-[4-[(4-Ethynylcyclohex-3-enyl)propylamino]butyl]biphenyl-4-carboxamide ((*R*)-1). To an ice-cooled solution of **8** (34.7 mg; 0.13 mmol) in CH_2Cl_2/DMSO (2 mL/1 mL) was added

Et_3N (72 µL; 0.516 mmol) and SO_3·pyridine (102.5 mg; 0.34 mmol). After stirring at room temperature for 1 h, the mixture was diluted with H_2O (10 mL) and extracted with EtOAc (4 x 20 mL). The combined organic layers were dried with $MgSO_4$ and concentrated. The resulting oil was diluted with CH_2Cl_2 (5 mL) and slowly added to an ice-cooled solution of **(*R*)-6** (7.5 mg; 0.05 mmol) in CH_2Cl_2 (5 mL). Then, $NaBH(OAc)_3$ (48.6 mg; 0.23 mmol) was added in one portion at 0 °C. The suspension was allowed to warm to room temperature and stirred for 4 h. The reaction was terminated by adding saturated aqueous $NaHCO_3$ and the aqueous layer was extracted with CH_2Cl_2. The combined organic layers were dried ($MgSO_4$) and the solvent was removed under reduced pressure. Purification of the resulting residue by HPLC (CH_3CN–H_2O + 0.1% HCOOH) yielded **(*R*)-1** as white solid (6.6 mg; 35%): analytical data according to the literature.[29] $[\alpha]^{26}_D$ = + 38.6° (*c* 0.4, MeOH). **(*S*)-1** (7.5 mg; 36%) $[\alpha]^{26}_D$ = - 40.4° (*c* 0.5, MeOH) was prepared from **(*S*)-6** as described above for **(*R*)-1**.

(*R*)-*N*-[4-[(4-Ethynylcyclohex-3-enyl)propylamino]butyl]pyrazolo[1,5-*a*]pyridine-2-carboxamide ((*R*)-2a). Compound **(*R*)-2a** was prepared according to the protocol of **(*R*)-1** using a solution of **9** (45.4 mg; 0.19 mmol) in CH_2Cl_2/DMSO (2 mL/1 mL), Et_3N (0.14 mL; 0.98 mmol) and SO_3·pyridine (237.8 mg; 0.78 mmol) as well as **(*R*)-6** (15.9 mg; 0.1 mmol) and $NaBH(OAc)_3$ (51.4 mg; 0.24 mmol). The crude compound was purified by flash chromatography (CH_2Cl_2 + 1–2% MeOH) to afford **(*R*)-2a** as yellowish oil (4.4 mg; 12%). IR: 3307, 2931, 1664, 1552, 1513, 1475, 1326, 1257, 1076, 804, 769, 740 cm^{-1}. ^{1}H-NMR (600 MHz, $CDCl_3$) δ 0.86 (t, *J* = 7.4 Hz, 3 H), 1.40-1.70 (m, 7 H), 1.84-1.89 (m, 1 H), 2.04-2.12 (m, 1 H), 2.18-2.30 (m, 3 H), 2.37-2.54 (m, 4 H), 2.77-2.84 (m, 2 H), 3.47-3.51 (m, 2 H), 6.13-6.16 (m, 1H), 6.85 (ddd, *J* = 1.4, 6.9, 6.9 Hz, 1 H), 7.05 (s, 1 H), 7.14 (ddd, *J* = 1.1, 6.7, 8.9 Hz, 1 H), 7.17-7.21 (m, 1 H), 7.58 (ddd, *J* = 1.2, 1.2, 8.9 Hz, 1 H), 8.37 (ddd, *J* = 1.1, 2.1, 7.1 Hz, 1 H). ^{13}C-NMR (360 MHz,

$CDCl_3$) δ 11.82, 21.82, 24.82, 26.10, 27.54, 28.19, 30.09, 39.12, 50.02, 52.40, 55.43, 74.86, 84.94, 97.88, 113.53, 119.24, 119.59, 123.63, 128.38, 135.51, 141.34, 148.03, 162.11. HR-EIMS calcd 378.2420; found 378.2419. $[\alpha]^{27}_D$ = + 29.4° (*c* 0.2, $CHCl_3$). **(*S*)-2a** (6.8mg; 16%) $[\alpha]^{27}_D$ = - 29.6° (*c* 0.5, $CHCl_3$) was prepared from **(*S*)-6** (18.4 mg; 0.11 mmol) as described above for **(*R*)-2a**.

(*R*)-*N*-[4-[(4-Ethynylcyclohex-3-enyl)propylamino]butyl]pyrazolo[1,5-*a*]pyridine-3-carboxamide ((*R*)-2b). Compound **(*R*)-2b** was prepared according to the protocol of **(*R*)-1** using a solution of **10** (124.6 mg; 0.53 mmol) in CH_2Cl_2/DMSO (2 mL/1 mL), Et_3N (0.37 mL; 2.67 mmol) and SO_3·pyridine (654.1 mg; 2.14 mmol) as well as **(*R*)-6** (28.9 mg; 0.18 mmol) and $NaBH(OAc)_3$ (93.7 mg; 0.44 mmol). The crude compound was purified by HPLC (MeOH–H_2O + 0.1% HCOOH) to afford **(*R*)-2b** as yellowish oil (5.4 mg; 8%). IR: 3308, 3094, 3026, 2930, 2862, 2806, 2092, 1637, 1555, 1531, 1468, 1442, 1367, 1334, 1273, 1247, 1218, 1175, 1151, 1123, 1078, 1011, 975, 919, 891, 828 cm^{-1}. ^{1}H-NMR (360 MHz, $CDCl_3$) δ 0.85 (t, *J* = 7.3 Hz, 3 H), 1.38-1.70 (m, 7 H), 1.81-1.88 (m, 1 H), 2.00-2.12 (m, 1 H), 2.15-2.29 (m, 3 H), 2.36-2.43 (m, 2 H), 2.49 (ddd, *J* = 1.9, 7.1, 7.1 Hz, 2 H), 2.75-2.83 (m, 2 H), 3.48 (ddd, *J* = 5.8, 7.0, 7.0 Hz, 2 H), 6.02-6.08 (m, 1H), 6.12-6.16 (m, 1 H), 6.91 (ddd, *J* = 1.5, 6.9, 6.9 Hz, 1 H), 7.34 (ddd, *J* = 1.1, 6.8, 8.9 Hz, 1 H), 8.12 (s, 1 H), 8.31 (ddd, *J* = 1.2, 1.2, 8.9 Hz, 1 H), 8.48 (ddd, *J* = 1.1, 1.1, 7.0 Hz, 1 H). ^{13}C-NMR (600 MHz, $CDCl_3$) δ 11.87, 22.05, 24.97, 26.51, 27.82, 28.28, 30.16, 39.33, 50.04, 52.54, 55.36, 74.82, 85.00, 106.95, 113.56, 119.60, 119.65, 126.31, 128.79, 135.63, 140.14, 140.62, 163.26. HR-EIMS calcd 378.2420; found 378.2420. $[\alpha]^{27}_D$ = + 24.2° (*c* 0.3, $CHCl_3$). **(*S*)-2b** (20.6mg; 39%) $[\alpha]^{27}_D$ = - 24.9° (*c* 1.7, $CHCl_3$) was prepared from **(*S*)-6** (22.5 mg; 0.14 mmol) as described above for **(*R*)-2b**.

(*R*)-4-[3-(1-Butyl-1*H*-1,2,3-triazol-4-yl)propoxy]-*N*-[4-[(6-ethynylcyclohex-3-enyl)propylamino]butyl]-3-methoxybenzamide ((*R*)-2c). Compound **(*R*)-2c** was prepared according to the protocol of **(*R*)-1** using a solution of **11** (74.8 mg; 0.19 mmol) in CH_2Cl_2/DMSO (2 mL/1 mL), Et_3N (0.13 mL; 0.93 mmol) and SO_3·pyridine (226.2 mg; 0.74 mmol) as well as **(*R*)-6** (12 mg; 0.074 mmol) and $NaBH(OAc)_3$ (47 mg; 0.22 mmol). The crude compound was purified by flash chromatography (CH_2Cl_2 + 1% MeOH) to afford **(*R*)-2c** as yellowish oil (25.6 mg; 63%). IR: 3286, 2933, 2108, 1637, 1581, 1544, 1506, 1465, 1268, 1224, 1130, 1029, 761 cm^{-1}. ^{1}H-NMR (360 MHz, $CDCl_3$) δ 0.87 (t, *J* = 7.3 Hz, 3 H), 0.94 (t, *J* = 7.3 Hz, 3 H), 1.20-1.38 (m, 2 H), 1.44-1.71 (m, 7 H), 1.81-1.97 (m, 3 H), 2.08-2.33 (m, 6 H), 2.43-2.64 (m, 4 H), 2.81 (s, 1 H), 2.85-2.97 (m, 3 H) 3.44-3.49 (m, 2 H), 3.92 (s, 3 H), 4.11 (t, *J* = 6.4 Hz, 2 H), 4.31 (t, *J* = 7.3 Hz, 2 H), 6.10-6.15 (m, 1 H), 6.53 (s, 1 H), 6.85 (d, *J* = 8.4 Hz, 1 H), 7.25-7.29 (m, 1 H), 7.30 (s, 1 H), 7.46 (d, *J* = 2.0 Hz, 1 H). ^{13}C-NMR (600 MHz, CD_3OD) δ 11.84, 13.43, 19.71, 21.83, 22.09, 24.89, 26.23, 27.53, 28.18, 28.67, 30.11, 32.29, 39., 49.90, 50.03, 52.47, 55.50, 56.13, 68.04, 74.94, 84.89, 111.21, 111.88, 119.11, 119.67, 120.80, 127.60, 135.37, 147.00, 149.37 151.08, 167.12. HR-EIMS calcd 549.3679; found 549.3681. $[\alpha]^{27}_D$ = + 18.9° (*c* 2.2, $CHCl_3$). **(*S*)-2c** (27.1mg; 64%) $[\alpha]^{27}_D$ = - 18.5° (*c* 1.3, $CHCl_3$) was prepared from **(*S*)-6** (12.6 mg; 0.08 mmol) as described above for **(*R*)-2c**.

(*R*)-*N*-[4-[(4-Ethynylcyclohex-3-enyl)propylamino]butyl]benzo[*b*]thiophene-2-carboxamide (*R*)-2d. Compound **(*R*)-2d** was prepared according to the protocol of **(*R*)-1** using a solution of **12** (33.9 mg; 0.16 mmol) in CH_2Cl_2/DMSO (2 mL/1 mL), Et_3N (0.11 mL; 0.8 mmol) and SO_3·pyridine (195.6 mg; 0.64 mmol) as well as **(*R*)-6** (13.1 mg; 0.08 mmol) and $NaBH(OAc)_3$ (42.4 mg; 0.2 mmol). The crude compound was purified by flash chromatography (CH_2Cl_2 + 2% MeOH) to afford **(*R*)-2d** as colorless oil (20.4 mg; 65%). IR: 3307, 3062, 3026,

2931, 2868, 2810, 2092, 1626, 1563, 1544, 1509, 1470, 1457, 1432, 1375, 1338, 1298, 1247, 1207, 1179, 1158, 1073, 974, 916, 868, 835 cm^{-1}. ^{1}H-NMR (600 MHz, $CDCl_3$) δ 0.86 (t, *J* = 7.4 Hz, 3 H), 1.41-1.63 (m, 7 H), 1.84-1.89 (m, 1 H), 2.05-2.13 (m, 1 H), 2.18-2.30 (m, 3 H), 2.38-2.55 (m, 4 H), 2.79-2.85 (m, 2 H), 3.45-3.51 (m, 2 H), 6.13-6.15 (m, 1 H), 6.47 (s, 1 H), 7.38-7.43 (m, 2 H), 7.77 (s, 1 H), 7.82-7.86 (m, 2 H). ^{13}C-NMR (600 MHz, $CDCl_3$) δ 11.85, 21.84, 24.92, 26.21, 27.46, 28.13, 30.12, 40.07, 49.97, 52.52, 55.51, 74.94, 84.89, 119.68, 122.69, 124.87, 124.97, 125.11, 126.22, 135.35, 138.65, 139.13, 140.73, 162.27. HR-EIMS calcd 394.2079; found 394.2079. $[\alpha]^{24}_{D}$ = + 35.8° (*c* 1.0, $CHCl_3$). **(*S*)-2d** (23.7 mg; 71%) $[\alpha]^{24}_{D}$ = -33.3° (*c* 0.7, $CHCl_3$) was prepared from **(*S*)-6** (13.9 mg; 0.085 mmol) as described above for **(*R*)-2d**.

(*R*)-*N*-[4-[(4-Ethynylcyclohex-3-enyl)propylamino]butyl]ferrocene carboxamide (*R*)-2e. Compound **(*R*)-2e** was prepared according to the protocol of **(*R*)-1** using a solution of **13** (33.5 mg; 0.11 mmol) in CH_2Cl_2/DMSO (2 mL/1 mL), Et_3N (80 μL; 0.56 mmol) and SO_3·pyridine (135.7 mg; 0.44 mmol) as well as **(*R*)-6** (13.1 mg; 0.08 mmol) and $NaBH(OAc)_3$ (42.4 mg; 0.2 mmol). The crude compound was purified by flash chromatography (hexane/EtOAc 2:1) to afford **(*R*)-2e** as orange solid (24.3 mg; 68%). Mp 98 °C. IR: 3309, 3093, 2926, 2854, 2093, 1725, 1630, 1541, 1456, 1436, 1377, 1342, 1300, 1219, 1180, 1105, 1075, 1024, 1001, 973, 915, 820 cm^{-1}. ^{1}H-NMR (360 MHz, $CDCl_3$) δ 0.87 (t, *J* = 7.3 Hz, 3 H), 1.38-1.64 (m, 7 H), 1.81-1.89 (m, 1 H), 2.00-2.13 (m, 1 H), 2.16-2.29 (m, 3 H), 2.36-2.52 (m, 4 H), 2.73-2.84 (m, 2 H), 3.35-3.41 (m, 2 H), 4.19 (s, 5 H), 4.33 (t, *J* = 1.9 Hz, 2 H), 4.64 (t, *J* = 1.9 Hz, 2 H), 5.74 (m, 1 H), 6.13-6.18 (m, 1 H). ^{13}C-NMR (600 MHz, $CDCl_3$) δ 11.88, 22.13, 25.01, 26.53, 27.91, 28.36, 30.18, 39.49, 50.06, 52.51, 55.35, 68.01, 69.69, 70.26, 74.81, 76.49, 85.02, 119.61, 135.69, 170.01. HR-EIMS calcd 446.2032; found 446.2031. $[\alpha]^{23}_{D}$ = + 30.8° (*c* 1.0, $CHCl_3$). **(*S*)-2e** (13.8

mg; 29%) $[\alpha]^{23}_{D}$ = - 28.4° (*c* 1.0, $CHCl_3$) was prepared from **(*S*)-6** (26.1 mg; 0.16) as described above for **(*R*)-2e**.

8-Ethynyl-1,4-dioxaspiro[4.5]decan-8-ol (3). To a diluted 0.5 molar solution of ethynylmagnesium bromide (154 mL; 52 mmol) in THF (50 mL) a solution of 1,4-dioxaspiro[4.5]decan-8-on (5.42 g; 34.7 mmol) in THF (20 mL) was added dropwise at 0 °C. This reaction mixture was continuously stirred for 2 h at room temperature. After addition of saturated aqueous NH_4Cl the mixture was extracted with Et_2O. The combined organic layers were dried over $MgSO_4$ and concentrated. The residue was purified by flash chromatography (hexane/EtOAc 3:1) to give **3** as a yellowish oil (5.69 g, 90% yield).[46] IR: 3430, 3284, 2956, 2884, 1702, 1436, 1367, 1253, 1162, 1105, 1033, 973, 773, 665, 549, 516 cm^{-1}. ^{1}H-NMR (600 MHz, $CDCl_3$) δ 1.76-1.84 (m, 4 H), 1.90-1.95 (m, 2 H), 1.96-2.02 (m, 3 H), 2.48 (s, 1 H), 3.95 (s, 4 H). ^{13}C-NMR (360 MHz, $CDCl_3$) δ 31.28, 37.04, 64.29, 64.34, 67.22, 72.04, 86.94, 107.83. HR-EIMS calcd 182.0943; found 182.0942.

4-Ethynyl-4-hydroxycyclohexanone (4). A solution of **3** (1.70 g; 9.33 mmol) and $CuSO_4$ (13 mg; 0.5 mol%) in 80% formic acid (6 mL) was stirred at room temperature for 16 h. After dilution with water, the mixture was alkalized with 6N NaOH and extracted with Et_2O. The combined organic layers were dried over $MgSO_4$ and evaporated. The residue was purified by flash chromatography (hexane/EtOAc 3:1) to give **4** as a white solid (1.02 g, 79% yield).[47] Mp 110 °C. IR: 3333, 3278, 2958, 1685, 1403, 1344, 1266, 1250, 1225, 1186, 1133, 1117, 1078, 953 cm^{-1}. ^{1}H-NMR (360 MHz, $CDCl_3$) δ 2.12-2.31 (m, 5 H), 2.45-2.61 (m, 5 H). ^{13}C-NMR (360 MHz, $CDCl_3$) δ 37.29, 38.77, 66.31, 73.13, 85.82, 209.54. HR-EIMS calcd 138.0681; found 138.0682.

1-Ethynyl-4-propylaminocyclohexan-1-ol (5). To an ice-cooled suspension of $NaBH(OAc)_3$ (5.68 g; 26.8 mmol) in CH_2Cl_2 (40 mL) a solution of **4** (1.48 g; 10.7 mmol) in CH_2Cl_2 (20 mL), propylamine (3.5 mL; 42.9 mmol) and glacial acetic acid (0.67 mL; 11.77 mmol) was added slowly. The mixture was allowed to warm to room temperature and stirred for 4 h. Then, the reaction was quenched with saturated aqueous $NaHCO_3$ and basified to pH 12 by 6N NaOH. The aqueous layer was extracted with CH_2Cl_2. The combined organic layers were dried ($MgSO_4$) and evaporated under reduced pressure. Purification by flash chromatography (CH_2Cl_2 + 5% MeOH saturated with NH_3) yielded **5** as a white solid (1.55 g; 80%). Mp 72 °C. IR: 3306, 2936, 2858, 2823, 2676, 2104, 1457, 1371, 1259, 1226, 1132, 1106, 1074, 969, 928, 907, 835 cm^{-1}. ^{1}H-NMR (360 MHz, $CDCl_3$) δ 0.92 (t, J = 7.4 Hz, 3 H), 1.41-1.64 (m, 5 H), 1.70-1.80 (m, 1 H), 1.89-2.05 (m, 4 H), 2.40-2.61 (m, 4 H). ^{13}C-NMR (360 MHz, $CDCl_3$) δ 11.82, 23.53, 28.00, 30.36, 36.90, 38.46, 49.27, 55.72, 73.02, 86.95. APCI-MS *m/z* 182 [M^++1].

4-Ethynyl-*N*-propylcyclohex-3-enamine (6). To a solution of **5** (1.32 g; 7.28 mmol), PPh_3 (5.73 g; 21.84 mmol) and imidazole (1.05 g; 15.43 mmol) in CH_2Cl_2 (60 mL) was added dropwise a solution of I_2 (3.81 g; 15 mmol) in CH_2Cl_2 (40 mL). The mixture was stirred at room temperature overnight. After addition of saturated aqueous $NaHCO_3$ and basification with 6N NaOH the organic layer was separated. The aqueous layer was extracted with CH_2Cl_2. The combined organic layers were dried ($MgSO_4$) and evaporated. The crude product was purified by flash chromatography (CH_2Cl_2 + 3% MeOH saturated with NH_3) to give **6** as a yellow oil (1.12 g; 94%). IR: 3310, 3030, 2957, 2926, 2823, 2874, 2093, 1373, 1302, 1226, 1124, 1058, 975, 912, 891, 835 cm^{-1}. ^{1}H-NMR (600 MHz, $CDCl_3$) δ 0.94 (t, J = 7.4 Hz, 3 H), 1.46-1.62 (m, 3 H), 1.91-2.05 (m, 2 H), 2.16-2.48 (m, 3 H), 2.60-2.69 (m, 2 H), 2.74-2.85 (m, 2 H), 3.64 (s, 1 H), 6.10-

6.14 (m, 1 H). ^{13}C-NMR (360 MHz, $CDCl_3$) δ 11.83, 23.55, 28.34, 28.79, 33.06, 49.04, 52.07, 74.93, 85.01, 119.68, 134.41. APCI-MS *m/z* 164 [M^++1].

The isolation of enantiopure **(*R*)-6** and **(*S*)-6** was accomplished by chiral resolution of racemic **6** employing HPLC separation with a Chiralpak AS-H column (1 cm x 25 cm; Chiral Technologies Europe) at a flow of 4.7 mL/min of CH_3CN + 0.1% $NHEt_2$: t_R = 4.7 min for **(*R*)-6** and t_R = 9.8 min for **(*S*)-6**. **(*R*)-6**: $[\alpha]^{27}_D$ = + 83.9° (*c* 0.8, $CHCl_3$). **(*S*)-6**: $[\alpha]^{27}_D$ = - 83.6° (*c* 0.8, $CHCl_3$).

(*S*)-*N*-(4-Ethynylcyclohex-3-enyl)-3,5-dinitro-*N*-propylbenzamide ((*S*)-7). To an ice-cooled solution of **(*S*)-6** (19.4 mg; 0.12 mmol) in CH_2Cl_2 (6 mL) was added dropwise Et_3N (66 µL; 0.48 mmol) and a solution of 3,5-dinitrobenzoyl chloride (32.9 mg; 0.14 mmol) in CH_2Cl_2 (3 mL). The reaction mixture was stirred at 0 °C for 4 h. After the addition of saturated $NaHCO_3$ solution, the organic layer was separated and the aqueous layer was extracted with CH_2Cl_2. The combined organic layers were dried ($MgSO_4$), evaporated and the residue was purified by flash chromatography (hexane/EtOAc 20:1 to 10:1). The obtained product was crystallized from a Et_2O/pentane solution to give **(*S*)-7** as yellow crystals (36.6 mg; 86%). IR: 3292, 3101, 2964, 2932, 2875, 2094, 1632, 1590, 1542, 1471, 1422, 1344, 1315, 1187, 1132, 1102, 1079, 1034, 978, 914, 815 cm^{-1}. ^{1}H-NMR (600 MHz, $CDCl_3$) δ 0.74 (t, *J* = 7.4 Hz, 0.9 H), 1.01 (t, *J* = 7.4 Hz, 2.1 H), 1.51-1.61 (m, 0.7 H), 1.69-1.81 (m, 1.4 H), 1.94-2.02 (m, 1.7 H), 2.06-2.24 (m, 1.7 H), 2.32-2.60 (m, 2.6 H), 2.88 (s, 0.7 H), 2.94 (s, 0.3 H), 3.14 (t, *J* = 8.1 Hz, 0.7 H), 3.28 (ddd, *J* = 5.2, 11.4, 13.2 Hz, 0.7 H), 3.40 (ddd, *J* = 5.2, 11.4, 13.2 Hz, 0.7 H), 3.54-3.60 (m, 0.7 H), 4.40-4.46 (m, 0.3 H), 6.05-6.08 (m, 0.7 H), 6.21-6.24 (m, 0.3 H), 8.59 (d, *J* = 2.1 Hz, 1.4 H), 8.63 (d, *J* = 2.1 Hz, 0.7 H), 9.18 (t, *J* = 2.1 Hz, 0.3 H), 9.19 (t, *J* = 2.1 Hz, 0.7 H); rotamers were observed. ^{13}C-NMR (600 MHz, $CDCl_3$) δ 11.24, 11.69, 22.23, 24.24, 25.98, 27.13, 28.77, 28.89, 29.32, 30.00, 44.07, 48.34, 51.55, 54.69, 75.67, 76.35, 83.29, 84.08, 119.09, 119.20, 11.32, 119.56,

126.62, 126.76, 132.79, 133.84, 139.77, 140.24, 147.88, 148.06, 166.26, 166.76; rotamers were observed. APCI-MS *m/z* 358.2 [M^++1]

***N*-[4-(Hydroxybutyl)]biphenyl-4-carboxamide (8)**

To an ice-cooled mixture of 4-aminobutanol (100 mg; 0.12 mmol) and aqueous NaOH (10%; 0.4 mL) in CH_2Cl_2 (1.2 mL) solution of biphenyl-4-carbonyl chloride (230 mg; 1.06 mmol) in CH_2Cl_2 (3 mL) was added dropwise, and the reaction was stirred at room temperature for 1 h. After addition of H_2O, the organic layer was separated and the aqueous layer was extracted with CH_2Cl_2. The combined organic layers were washed with 2N-HCl, H_2O and saturated aqueous NaCl, dried ($MgSO_4$) and evaporated under reduced pressure. The resulting white solid **8** (263.3 mg; 92%) was used without further purification. Analytical data according to the literature.[48]

***N*-(4-Hydroxybutyl)pyrazolo[1,5-*a*]pyridine-2-carboxamide (9).** A solution of pyrazolo[1,5-*a*]pyridine-2-carboxylic acid (121.5 mg; 0.75 mmol) and carbonyldiimidazole (182.3 mg; 1.12 mmol) in DMF (10 mL) was stirred at 50 °C for 2 h. After cooling to room temperature and dropwise addition of 4-aminobutanol (0.21 mL; 2.25 mmol), the reaction mixture was stirred at room temperature for 2 h. Then, saturated aqueous NaCl solution was added, the aqueous layer was neutralized with aqueous HCl and extracted with CH_2Cl_2. The combined organic layers were dried ($MgSO_4$) and evaporated. Purification of the residue by flash chromatography (CH_2Cl_2 + 3% MeOH) yielded **9** as a white solid (131.2 mg; 75%). Mp 60 °C. IR: 3398, 3325, 3090, 3034, 2936, 2866, 1651, 1557, 1514, 1476, 1423, 1327, 1259, 1145, 1052, 842, 806 cm^{-1}. ^{1}H-NMR (600 MHz, $CDCl_3$) δ 1.67-1.78 (m, 4 H), 3.54 (dd, *J* = 6.9, 13.1 Hz, 2 H), 3.73 (t, *J* = 6.2 Hz, 2 H), 6.85 (ddd, *J* = 1.4, 6.9, 6.9 Hz, 1 H), 7.14 (ddd, *J* = 1.1, 6.6, 8.9 Hz, 1 H), 7.24 (s, 1 H), 7.58 (ddd, *J* = 1.3, 1.3, 8.9 Hz, 1 H), 8.37 (ddd, *J* = 1.1, 2.1, 6.9 Hz, 1 H).

^{13}C-NMR (600 MHz, $CDCl_3$) δ 26.32, 29.81, 38.98, 62.48, 97.93, 113.58, 119.26, 123.68, 128.38, 141.36, 147.95, 162.29. APCI-MS *m/z* 234.0 [M^+ + 1].

***N*-(4-Hydroxybutyl)pyrazolo[1,5-*a*]pyridine-3-carboxamide (10).** Compound **10** was prepared according to the protocol of **9** using a solution of pyrazolo[1,5-*a*]pyridine-3-carboxylic acid (114.5 g; 0.71 mmol) and carbonyldiimidazole (171.8 g; 1.1 mmol) in DMF (10 mL) as well as 4-aminobutanol (0.2 mL; 2.12 mmol). The crude compound was purified by flash chromatography (CH_2Cl_2 + 2% MeOH) to afford **10** as white solid (107 mg; 65%). IR: 3326, 2938, 2867, 1650, 1558, 1514, 1476, 1424, 1328, 1260, 1145, 1052, 843 cm^{-1}. ^{1}H-NMR (600 MHz, $CDCl_3$) δ 1.68-1.79 (m, 4 H), 3.50-3.54 (m, 2 H), 3.75 (t, J = 6.0 Hz, 2 H), 6.64 (s, 1 H), 6.91 (ddd, *J* = 1.6, 6.9, 6.9 Hz, 1 H), 7.34 (ddd, *J* = 1.1, 6.6, 8.9 Hz, 1 H), 8.19 (s, 1 H), 8.31 (ddd, *J* = 1.0, 1.0, 8.9 Hz, 1 H), 8.48 (ddd, *J* = 1.0, 1.0, 6.9, 1 H). APCI-MS *m/z* 234.0 [M^++1].

4-[3-(1-Butyl-1*H*-1,2,3-triazol-4-yl)propoxy]-*N*-(4-hydroxybutyl)-3-methoxybenzamide (11). Compound **11** was prepared according to the protocol of **9** using a solution of 4-[3-(1-butyl-1*H*-1,2,3-triazol-4-yl)propoxy]-3-methoxybenzoic acid (182.5 mg; 0.55 mmol) and carbonyldiimidazole (133 mg; 0.82 mmol) in DMF (10 mL) as well as 4-aminobutanol (0.15 mL; 1.64 mmol). The crude compound was purified by flash chromatography (CH_2Cl_2 + 3% MeOH) to afford **11** as white solid (209.1 mg; 94%). Mp 105 °C. IR: 3437, 3342, 3121, 3066, 2942, 2873, 1627, 1598, 1578, 1532, 1509, 1469, 1415, 1395, 1335, 1296, 1275, 1228, 1190, 1153, 1132, 1097, 1057, 1032, 997, 944, 874, 816 cm^{-1}. ^{1}H-NMR (360 MHz, $CDCl_3$) δ 0.94 (t, *J* = 7.3 Hz, 3 H), 1.28-1.40 (m, 2 H), 1.62-1.90 (m, 6 H), 2.11 (s, 1 H), 2.19-2.27 (m, 2 H), 2.92 (t, *J* = 7.4 Hz, 2 H), 3.46-3.51 (m, 2 H), 3.73 (t, *J* = 6.0 Hz, 2 H), 3.90 (s, 3H), 4.09 (t, *J* = 6.4 Hz, 2 H), 4.30 (t, *J* = 7.2 Hz, 2 H), 6.59 (t, *J* = 5.7 Hz, 1 H), 6.83 (d, *J* = 8.3 Hz, 1 H), 7.24 (dd, *J* = 2.0, 8.3 Hz, 1 H), 7.31 (s, 1 H), 7.44 (d, *J* = 2.0 Hz, 1 H). ^{13}C-NMR (360 MHz, $CDCl_3$) δ 13.41, 19.68,

22.05, 26.37, 28.65, 29.84, 32.25, 39.79, 49.91, 56.06, 62.42, 67.99, 111.13, 111.88, 119.22, 120.85, 127.46, 146.98, 149.29, 151.02, 167.21.

***N*-(4-Hydroxybutyl)benzo[*b*]thiophene-2-carboxamide (12).** Compound **12** was prepared according to the protocol of **9** using a solution of benzo[*b*]thiophene-2-carboxylic acid (327 mg; 1.84 mmol) and carbonyldiimidazole (446.3 mg; 2.75 mmol) in DMF (20 mL) as well as 4-aminobutanol (0.52 mL; 5.52 mmol). The crude compound was purified by flash chromatography (CH_2Cl_2 + 3% MeOH) to afford **12** as white solid (333.6 mg; 73%). Analytical data according to the literature.[49,50]

***N*-(4-Hydroxybutyl)ferrocene carboxamide (13).** Compound **13** was prepared according to the protocol of **9** using a solution of ferrocene carboxylic acid (164.1 mg; 0.71 mmol) and carbonyldiimidazole (173.5 mg; 1.07 mmol) in DMF (10 mL) as well as 4-aminobutanol (0.2 mL; 2.13 mmol). The crude compound was purified by flash chromatography (CH_2Cl_2 + 4% MeOH) to afford **13** as orange solid (124 mg; 58%). IR: 3311, 3094, 2929, 2858, 1777, 1698, 1625, 1542, 1446, 1376, 1301, 1189, 1105, 1054, 1031, 1007, 813 cm^{-1}. ^{1}H-NMR (600 MHz, $CDCl_3$) δ 1.65-1.74 (m, 4 H), 1.90 (t, J = 5.2 Hz, 1 H), 3.41-3.45 (m, 2 H), 3.73-3.76 (m, 2 H), 4.20 (s, 5 H), 4.33 (t, J = 1.9 Hz, 2 H), 4.66 (t, J = 1.9 Hz, 2 H), 5.99 (m, 1 H). APCI-MS *m/z* 302.1 [M^++1].

Metabolism studies. Pooled microsomes from male rat liver (spargue-Dawley) were purchased from Sigma Aldrich and stored at – 75 °C until required. NADPH was purchased from Carl Roth and stored at – 8 °C. The incubation reactions were carried out in polyethylene cups (Eppendorf®, 1.5 mL) in a water bath at 37 °C. The incubation mixture contained 0.05 mg/mL test compound **1** or rotigotine, pooled rat liver microsomes (sprague-Dawley rats, male; 1 mg micosomal protein/mL incubation mixture) and Tris-$MgCl_2$ buffer (24 mM Tris, 2.4 mM $MgCl_2$,

pH 7.4). The final volume was 1 mL. The microsomal reactions were initiated by the addition of 100 µL enzyme cofactor solution NADPH (final concentration of 1 mM). Aliquotes (150 µL each) were drawn after predetermined time intervals of 0, 15, 30, 45 and 60 min, the enzymatic reactions were terminated by addition of 150 µL ice-cold CH_3OH (containing 0.87 mM internal standard) and precipitated protein was removed by centrifugation. The supernatant was analyzed by HPLC and HPLC/MS (binary solvent system: eluent CH_3OH in 0.1% aqueous formic acid, 20% to 80% CH_3OH in 15 min, 80% to 100% in 1 min, 100% for 5 min, flow rate 0.5 mL/min, λ 254 nm and 220 nm). All incubations were performed in duplicate, parallel control incubations were conducted in the absence of microsomal protein or cofactor solution.

Receptor Binding Studies. Receptor binding studies were carried out as described previously.[25, 51] In brief, the dopamine D_1 receptor assay was done with porcine striatal membranes at a final protein concentration of 20-30 µg/assay tube and the radioligand [^{3}H]SCH 23390 (specific activity = 60 Ci/mmol, Biotrend, Cologne, Germany) at 0.50 nM (K_D = 0.56-0.67 nM, B_{max} = 420-625 fmol/mg protein). For competition binding experiments with the human D_{2L}, D_{2S},[52] D_3[53] and $D_{4.4}$[54] receptors preparations of membranes from CHO cells stably expressing the corresponding receptor were used together with [^{3}H]spiperone (specific activity = 81 Ci/mmol, PerkinElmer, Rodgau, Germany) at a final concentration of 0.10-0.30 nM. The assays were carried out at a protein concentration of 2-10 µg/assay tube, K_D values of 0.036-0.12 nM, 0.040-0.11 nM, 0.12-0.30 nM, and 0.17-0.26 nM and corresponding B_{max} values of 640-1310 fmol/mg, 2130-4800 fmol/mg, 2340-6450 fmol/mg, and 630-2170 fmol/mg for the D_{2L}, D_{2S}, D_3 and $D_{4.4}$ receptors, respectively. Competition binding experiments exclusively labeling the high affinity binding site of the D_{2L} receptor were performed as described above with the difference that the assays were run in 24-well plates at a final volume of 500 µl/well. The agonist

radioligand [^{3}H]7-OH-DPAT (specific activity = 160 Ci/mmol, custom synthesis by Biotrend, Cologne, Germany) was incubated at a concentration of 1.0 nM with membranes at a final concentration of 15-50 µg/assay tube, K_D values of 0.87-2.0 nM and B_{max} values of 145-385 fmol/mg. Binding studies with the porcine serotonin and adrenergic receptors were carried out as described.[25, 55] Homogenates from porcine cerebral cortex were prepared and assays were run with membranes at a protein concentration per each assay tube of 60-100 µg/mL, 80 µg/mL and 30-60 µg/mL for 5-HT_{1A}, 5-HT_2 and α1, respectively, in the presence of the radioligands [^{3}H]WAY100635 (specific activity = 80 Ci/mmol, Biotrend, Cologne, Germany) (0.15-0.20 nM final concentration, K_D = 0.048-0.087 nM, B_{max} = 40-80 fmol/mg), [^{3}H]ketanserin (specific activity = 53 Ci/mmol, PerkinElmer, Rodgau, Germany) (0.50 nM final concentration, K_D = 1.9-2.2 nM, B_{max} = 130-150 fmol/mg) and [^{3}H]prazosin (specific activity = 83 Ci/mmol, PerkinElmer, Rodgau, Germany) (0.20 nM final concentration, K_D = 0.070-0.14 nM, B_{max} = 75-180 fmol/mg), respectively. Protein concentration was established by the method of Lowry using bovine serum albumin as standard.[56]

[^{35}S]GTPγS Incorporation Assay. The [^{35}S]GTPγS binding assay was performed on membrane preparation of transiently transfected HEK-293 cells that expressed the corresponding dopamine receptor and the appropriate pertussin toxin insensitive Gα protein (D_{2L} + $G\alpha_{o1}$, D_{2L} + $G\alpha_{i2}$ or D_{2S} + $G\alpha_{o1}$, D_{2S} + $G\alpha_{i2}$) as describe previously.[51] In brief, membranes (30 µg/mL of membrane protein), compounds and 10 µM GDP were preincubated in the absence of [^{35}S]GTPγS for 30 min at 37°C. After the addition of 0.10 nM [^{35}S]GTPγS (specific activity = 1250 Ci/mmol, PerkinElmer, Rodgau, Germany), membranes were incubated for additional 30 min (D_2 + $G\alpha_{o1}$) or 75 min (D_2 + $G\alpha_{i2}$) at 37°C. Reactions were terminated by filtration through Whatman GF/B filters soaked with ice cold PBS. The filter-bound radioactivity was measured as

described above. Three to six experiments per compound were performed with each concentration in triplicates.

β-Arrestin Recruitment Assay. The measurement of β-arrestin recruitment stimulated by receptor activation was performed utilizing the PathHunter® assay purchased from DiscoveRx (DiscoveRx, Birmingham, UK) according to the manufacturer's protocol. In brief, HEK-239 cells stably expressing the Enzyme acceptor (EA)-tagged β-Arrestin fusion protein were transiently transfected with the ProLink® (PK2)-tagged dopamine receptor D_{2S} using the TransIT®-293 transfection reagent from Mirus (purchased from MoBiTec, Goettingen, Germany). Cells (5000 cells per well) were seeded in 384-well plates and incubated for 24 hrs. After incubation with 10 μM (final concentration) of test compounds in triplicates for 20 hrs the detection mix was added and incubation was continued for further 60 min. Chemiluminescence was determined with a plate reader for microplates (Victor^3-V, PerkinElmer, Rodgau, Germany).

Data Analysis. The resulting competition curves of the receptor binding experiments were analyzed by nonlinear regression using the algorithms in PRISM 5.0 (GraphPad Software, San Diego, CA). The data were initially fit using a sigmoid model to provide an IC_{50} value, representing the concentration corresponding to 50% of maximal inhibition. IC_{50} values were transformed to K_i values according to the equation of Cheng and Prusoff.[57]

Dose-response curves on [^{35}S]GTPγS binding were normalized to basal binding of radioactivity (= 0%) and the effect of the full agonist and reference compound quinpirole (maximum effect = 100%). Three to six curves each representing individual experiments were pooled to a mean curve from which the maximum activity could be derived. For the calculation of the functional selectivity index FSI each dose-response curve was analyzed in the range of 0.1

nM to 100 μM to get the area under the curve (AUC) using the algorithms in PRISM 5.0. The FSI for a particular test compound at a particular receptor subtype was created when calculating the difference between the AUC for the system D_2+$G\alpha_{o1}$ and that of D_2+$G\alpha_{i2}$ in relation to the effect of quinpirole according to the formula:

$$FSI = (\Delta AUC[test(G\alpha_o\text{-}G\alpha_i)] - \Delta AUC[ref(G\alpha_o\text{-}G\alpha_i)]) / \Delta AUC[ref(G\alpha_o\text{-}G\alpha_i)]$$

resulting in positive values for FSI indicating functional selectivity of D_2+$G\alpha_{o1}$ over D_2+$G\alpha_{i2}$ and negative values displaying functional selectivity of D_2+$G\alpha_{i2}$ over D_2+$G\alpha_{o1}$.

The amount of recruitment of β-arrestin was derived from the agonist induced increase of chemiluminescence, which was expressed in CPS (counts per second). These data were normalized to the basal effect of buffer (PBS) equal to 0% and 100 % to the effect of the full agonist and reference compound quinpirole.

Homology modeling. We used the crystal structure of the D_3 receptor[43] (PDB-ID: 3PBL) as a template to create a homology model of the D_2 receptor. The amino-acid sequences of D_2 and D_3 were retrieved from the SWISS-PROT database.[58] Together with 16 additional sequences of family A GPCRs, the D_2 and D_3 sequences were aligned using ClustalX[59] (Gonnet series matrix with a gap open penalty of 10 and a gap extension penalty of 0.2). The initial sequence alignment was manually refined where necessary by means of BioEdit[60] in order to achieve a perfect alignment of the highly conserved amino acids. Absent parts of the D_3 crystal structure, especially the third intracellular loop, were omitted in the alignment. Based on the final alignment and the crystal structure of the D_3 receptor as a template, we created 100 models of the D_2 receptor using MODELLER 9v4.[61] One model with serine residues 5.42 and 5.43 pointing towards the interior of the helical bundle was selected manually and used for the docking investigations.

Molecular Docking. The ligands quinpirole and **(*S*)-2c** were geometry optimized by means of Gaussian 09[62] at the HF/6-31(d,p) level (attributing a formal charge of +1) and subsequently docked into the D_2 model using AutoDock Vina.[63] We applied a search space of 22 x 26 x 30 Å to ensure a complete coverage of the binding pocket. The ligands were subjected to the docking procedure using an exhaustiveness value of 32 and a randomly selected starting position. 20 conformations of each ligand were obtained and inspected manually. On the basis of the scoring function of AutoDock Vina and experimental data, we selected one final conformation for each ligand.

Both ligand-receptor complexes were subsequently submitted to energy minimization using the SANDER module of the AMBER10 program package.[64] The all-atom force field ff99SB[65] and the general AMBER force field (GAFF)[66] were used for D_2 and the ligands, respectively. Parameters for quinpirole and **(*S*)-2c** were assigned using antechamber[64] and charges were calculated using Gaussian 09 at the HF/6-31(d,p) level and the RESP procedure according to the literature.[67] A formal charge of +1 was defined for the ligands. We applied 2,500 steps of steepest descent minimization, followed by 7,500 steps of conjugate gradient minimization. The minimization steps were carried out in a water box with periodic boundary conditions and a nonbonded cutoff of 10.0 Å.

ASSOCIATED CONTENT

Supporting Information. NMR spectra, HPLC purity data including spectra, X-ray crystal structure data and results of functional assays. This material is available free of charge via the Internet at http://pubs.acs.org.

ACKNOWLEDGMENT

The German Science Foundation (DFG) is acknowledged for financial support. We thank Prof. Graeme Milligan (University of Glasgow, U.K.) for providing us with the cDNA for $G\alpha_{o1}$ or $G\alpha_{i2}$ proteins as well as Dr. Nuska Tschammer and Tizita Haimanot Admas fort the construction of (PK2)-tagged dopamine receptor cDNA.

* To whom correspondence should be addressed. Mailing address: Department of Chemistry and Pharmacy, Emil Fischer Center, Friedrich Alexander University, Schuhstr. 19, 91052 Erlangen, Germany. Tel: +49 9131 85-29383. Fax: +49 9131 85-22585. Email: peter.gmeiner@fau.de

[a]**Abbreviations:** aripiprazole, 7-[4-[4-(2,3-dichlorophenyl)piperazin-1-yl]butoxy]-3,4-dihydroquinolin-2(1*H*)-one; MAP kinase, mitogen-activated protein kinase; D_x, dopamine D_x receptor; ERK, extracellular signal-regulated kinases; GTPγS, guanosine 5'-*O*-(thiotriphosphate); CDI, carbonyldiimidazole; ropinirole, 4-[2-(dipropylamino)ethyl]-1,3-dihydro-2*H*-indol-2-one; rotigotine, (*S*)-2-(*N*-propyl-*N*-2-thienylethylamino)-5-hydroxytetralin; spiperone, 8-[4-(4-fluorophenyl)-4-oxobutyl]-1-phenyl-1,3,8-triazaspiro[4.5]decan-4-one; CHO, chinese hamster ovary; SEM, standard error of mean; ketanserin, 3-[2-[4-(4-fluorobenzoyl)piperidin-1-yl]ethyl]quinazoline-2,4(1*H*,3*H*)-dione; prazosin, 2-[4-(2-

furoyl)piperazin-1-yl]-6,7-dimethoxyquinazolin-4-amine; PTX, pertussis toxin; quinpirole, (4a*R*-trans)-4,4a,5,6,7,8,8a,9-octahydro-5-propyl-1*H*-pyrazolo[3,4-*g*]quinoline; APCI, atmospheric pressure chemical ionization.

References

1. Neve, K. A. *Functional Selectivity of G Protein-Coupled Receptor Ligands*. 1st ed.; Humana Press: Totowa, NJ, 2009; p 25-40.

2. Wei, H.; Ahn, S.; Shenoy, S. K.; Karnik, S. S.; Hunyady, L.; Luttrell, L. M.; Lefkowitz, R. J. Independent beta-arrestin 2 and G protein-mediated pathways for angiotensin II activation of extracellular signal-regulated kinases 1 and 2. *Proc. Natl. Acad. Sci. U.S.A.* **2003**, *100*, 10782-10787.

3. Lefkowitz, R. J.; Shenoy, S. K. Transduction of receptor signals by beta-arrestins. *Science* **2005**, *308*, 512-517.

4. Liu, J. J.; Horst, R.; Katritch, V.; Stevens, R. C.; Wuthrich, K. Biased signaling pathways in beta2-adrenergic receptor characterized by 19F-NMR. *Science* **2012**, *335*, 1106-1110.

5. Wacker, D.; Wang, C.; Katritch, V.; Han, G. W.; Huang, X. P.; Vardy, E.; McCorvy, J. D.; Jiang, Y.; Chu, M.; Siu, F. Y.; Liu, W.; Xu, H. E.; Cherezov, V.; Roth, B. L.; Stevens, R. C. Structural features for functional selectivity at serotonin receptors. *Science* **2013**, *340*, 615-619.

6. Allen, J. A.; Yost, J. M.; Setola, V.; Chen, X.; Sassano, M. F.; Chen, M.; Peterson, S.; Yadav, P. N.; Huang, X. P.; Feng, B.; Jensen, N. H.; Che, X.; Bai, X.; Frye, S. V.; Wetsel, W. C.; Caron, M. G.; Javitch, J. A.; Roth, B. L.; Jin, J. Discovery of beta-arrestin-biased dopamine D2 ligands for probing signal transduction pathways essential for antipsychotic efficacy. *Proc. Natl. Acad. Sci. U.S.A.* **2011**, *108*, 18488-18493.

7. Chen, X.; Sassano, M. F.; Zheng, L.; Setola, V.; Chen, M.; Bai, X.; Frye, S. V.; Wetsel, W. C.; Roth, B. L.; Jin, J. Structure-functional selectivity relationship studies of beta-arrestin-biased dopamine D(2) receptor agonists. *J. Med. Chem.* **2012**, *55*, 7141-7153.

8. Masri, B.; Salahpour, A.; Didriksen, M.; Ghisi, V.; Beaulieu, J. M.; Gainetdinov, R. R.; Caron, M. G. Antagonism of dopamine D2 receptor/beta-arrestin 2 interaction is a common property of clinically effective antipsychotics. *Proc. Natl. Acad. Sci. U.S.A.* **2008**, *105*, 13656-13661.

9. Strange, P. G. Antipsychotic drugs: importance of dopamine receptors for mechanisms of therapeutic actions and side effects. *Pharmacol. Rev.* **2001**, *53*, 119-133.

10. Joyce, J. N.; Millan, M. J. Dopamine D3 receptor antagonists as therapeutic agents. *Drug Discov. Today* **2005**, *10*, 917-925.

11. Zhang, A.; Neumeyer, J. L.; Baldessarini, R. J. Recent progress in development of dopamine receptor subtype-selective agents: potential therapeutics for neurological and psychiatric disorders. *Chem. Rev.* **2007**, *107*, 274-302.

12. Heidbreder, C. A.; Newman, A. H. Current perspectives on selective dopamine D(3) receptor antagonists as pharmacotherapeutics for addictions and related disorders. *Ann. N. Y. Acad. Sci.* **2010**, *1187*, 4-34.

13. Beaulieu, J. M.; Gainetdinov, R. R. The physiology, signaling, and pharmacology of dopamine receptors. *Pharmacol. Rev.* **2011**, *63*, 182-217.

14. Lane, J. R.; Powney, B.; Wise, A.; Rees, S.; Milligan, G. G protein coupling and ligand selectivity of the D2L and D3 dopamine receptors. *J. Pharmacol. Exp. Ther.* **2008**, *325*, 319-330.

15. Gazi, L.; Nickolls, S. A.; Strange, P. G. Functional coupling of the human dopamine D2 receptor with G alpha i1, G alpha i2, G alpha i3 and G alpha o G proteins: evidence for agonist regulation of G protein selectivity. *Br. J. Pharmacol.* **2003**, *138*, 775-786.

16. Jiang, M.; Spicher, K.; Boulay, G.; Wang, Y.; Birnbaumer, L. Most central nervous system D2 dopamine receptors are coupled to their effectors by Go. *Proc. Natl. Acad. Sci. U.S.A.* **2001**, *98*, 3577-3582.

17. Jiang, M.; Bajpayee, N. S. Molecular mechanisms of go signaling. *Neurosignals* **2009**, *17*, 23-41.

18. Liu, Y. F.; Jakobs, K. H.; Rasenick, M. M.; Albert, P. R. G protein specificity in receptor-effector coupling. Analysis of the roles of G0 and Gi2 in GH4C1 pituitary cells. *J. Biol. Chem.* **1994**, *269*, 13880-13886.

19. Ghahremani, M. H.; Cheng, P.; Lembo, P. M.; Albert, P. R. Distinct roles for Galphai2, Galphai3, and Gbeta gamma in modulation offorskolin- or Gs-mediated cAMP accumulation and calcium mobilization by dopamine D2S receptors. *J. Biol. Chem.* **1999**, *274*, 9238-9245.

20. Ghahremani, M. H.; Forget, C.; Albert, P. R. Distinct roles for Galpha(i)2 and Gbetagamma in signaling to DNA synthesis and Galpha(i)3 in cellular transformation by dopamine D2S receptor activation in BALB/c 3T3 cells. *Mol. Cell. Biol.* **2000**, *20*, 1497-1506.

21. Quan, W.; Kim, J. H.; Albert, P. R.; Choi, H.; Kim, K. M. Roles of G protein and beta-arrestin in dopamine D2 receptor-mediated ERK activation. *Biochem. Biophys. Res. Commun.* **2008**, *377*, 705-709.

22. Cordeaux, Y.; Nickolls, S. A.; Flood, L. A.; Graber, S. G.; Strange, P. G. Agonist regulation of D(2) dopamine receptor/G protein interaction. Evidence for agonist selection of G protein subtype. *J. Biol. Chem.* **2001**, *276*, 28667-28675.

23. Lober, S.; Hubner, H.; Tschammer, N.; Gmeiner, P. Recent advances in the search for D3- and D4-selective drugs: probes, models and candidates. *Trends Pharmacol. Sci.* **2011**, *32*, 148-157.

24. Tschammer, N.; Bollinger, S.; Kenakin, T.; Gmeiner, P. Histidine 6.55 is a major determinant of ligand-biased signaling in dopamine D2L receptor. *Mol. Pharmacol.* **2011**, *79*, 575-585.

25. Hubner, H.; Haubmann, C.; Utz, W.; Gmeiner, P. Conjugated enynes as nonaromatic catechol bioisosteres: Synthesis, binding experiments, and computational studies of novel dopamine receptor agonists recognizing preferentially the D-3 subtype. *J. Med. Chem.* **2000**, *43*, 756-762.

26. Lenz, C.; Boeckler, F.; Hubner, H.; Gmeiner, P. Analogues of FAUC 73 revealing new insights into the structural requirements of nonaromatic dopamine D3 receptor agonists. *Bioorg. Med. Chem.* **2004**, *12*, 113-117.

27. Lenz, C.; Haubmann, C.; Hubner, H.; Boeckler, F.; Gmeiner, P. Fancy bioisosteres: synthesis and dopaminergic properties of the endiyne FAUC 88 as a novel non-aromatic D3 agonist. *Bioorg. Med. Chem.* **2005**, *13*, 185-191.

28. Lenz, C.; Boeckler, F.; Hubner, H.; Gmeiner, P. Fancy bioisosteres: synthesis, SAR, and pharmacological investigations of novel nonaromatic dopamine D3 receptor ligands. *Bioorg. Med. Chem.* **2005**, *13*, 4434-4442.

29. Dorfler, M.; Tschammer, N.; Hamperl, K.; Hubner, H.; Gmeiner, P. Novel D3 Selective Dopaminergics Incorporating Enyne Units as Nonaromatic Catechol Bioisosteres: Synthesis, Bioactivity, and Mutagenesis Studies. *J. Med. Chem.* **2008**, *51*, 6829-6838.

30. Lange, G. L.; Gottardo, C. Facile Conversion of Primary and Secondary Alcohols to Alkyl Iodides. *Synthetic Commun.* **1990**, *20*, 1473-1479.

31. Pouwer, R. H.; Schill, H.; Williams, C. M.; Bernhardt, P. V. Investigating direct access to 2-oxospiro[4.5]decanones via 6 pi-electrocyclisation. *Eur. J. Org. Chem.* **2007**, 4699-4705.

32. Kuhhorn, J.; Gotz, A.; Hubner, H.; Thompson, D.; Whistler, J.; Gmeiner, P. Development of a Bivalent Dopamine D2 Receptor Agonist. *J. Med. Chem.* **2011**, *54*, 7911-7919.

33. Parikh, J. R.; Doering, W. v. E. Sulfur trioxide in the oxidation of alcohols by dimethyl sulfoxide. *J. Am. Chem. Soc.* **1967**, *89*, 5505-5507.

34. Bloomer, J. C.; Clarke, S. E.; Chenery, R. J. In vitro identification of the P450 enzymes responsible for the metabolism of ropinirole. *Drug Metab. Dispos.* **1997**, *25*, 840-844.

35. Ramji, J. V.; Keogh, J. P.; Blake, T. J.; Broom, C.; Chenery, R. J.; Citerone, D. R.; Lewis, V. A.; Taylor, A. C.; Yeulet, S. E. Disposition of ropinirole in animals and man. *Xenobiotica* **1999**, *29*, 311-325.

36. Cawello, W.; Braun, M.; Boekens, H. Absorption, Disposition, Metabolic Fate, and Elimination of the Dopamine Agonist Rotigotine in Man: Administration by Intravenous Infusion or Transdermal Delivery. *Drug Metab. Dispos.* **2009**, *37*, 2055-2060.

37. Swart, P. J.; Oelen, W. E. M.; Bruins, A. P.; Tepper, P. G.; Dezeeuw, R. A. Determination of the Dopamine-D2 Agonist N-0923 and Its Major Metabolites in Perfused Rat Livers by Hplc Uv Atmospheric-Pressure Ionization Mass-Spectrometry. *J. Anal. Toxicol.* **1994**, *18*, 71-77.

38. Hubble, J. P. Pre-clinical studies of pramipexole: clinical relevance. *Eur. J. Neurol.* **2000**, *7*, 15-20.

39. Koble, D. L.; Koons, J. C.; Fischer, L. J. Metabolism and Disposition of the Dopaminergic Agonist 5-Hydroxy-6-Methyl-2-Di-Normal-Propylaminotetralin in the Rat. *Drug Metab. Dispos.* **1985**, *13*, 305-311.

40. Vyas, K. P.; Kari, P. H.; Ramjit, H. G.; Pitzenberger, S. M.; Hichens, M. Metabolism of Antiparkinson Agent Dopazinol by Rat-Liver Microsomes. *Drug Metab. Dispos.* **1990**, *18*, 1025-1030.

41. Millan, M. J.; Maiofiss, L.; Cussac, D.; Audinot, V.; Boutin, J. A.; Newman-Tancredi, A. Differential actions of antiparkinson agents at multiple classes of monoaminergic receptor. I. A multivariate analysis of the binding profiles of 14 drugs at 21 native and cloned human receptor subtypes. *J. Pharmacol. Exp. Ther.* **2002**, *303*, 791-804.

42. Senogles, S. E. The D2 dopamine receptor isoforms signal through distinct Gi alpha proteins to inhibit adenylyl cyclase. A study with site-directed mutant Gi alpha proteins. *J. Biol. Chem.* **1994**, *269*, 23120-23127.

43. Chien, E. Y.; Liu, W.; Zhao, Q.; Katritch, V.; Han, G. W.; Hanson, M. A.; Shi, L.; Newman, A. H.; Javitch, J. A.; Cherezov, V.; Stevens, R. C. Structure of the human dopamine D3 receptor in complex with a D2/D3 selective antagonist. *Science* **2010**, *330*, 1091-1095.

44. Rosenkilde, M. M.; Benned-Jensen, T.; Frimurer, T. M.; Schwartz, T. W. The minor binding pocket: a major player in 7TM receptor activation. *Trends Pharmacol. Sci.* **2010**, *31*, 567-574.

45. Wang, C.; Jiang, Y.; Ma, J.; Wu, H.; Wacker, D.; Katritch, V.; Han, G. W.; Liu, W.; Huang, X. P.; Vardy, E.; McCorvy, J. D.; Gao, X.; Zhou, X. E.; Melcher, K.; Zhang, C.; Bai, F.; Yang, H.; Yang, L.; Jiang, H.; Roth, B. L.; Cherezov, V.; Stevens, R. C.; Xu, H. E. Structural basis for molecular recognition at serotonin receptors. *Science* **2013**, *340*, 610-614.

46. Magnus, P.; Carter, P.; Elliott, J.; Lewis, R.; Harling, J.; Pitterna, T.; Bauta, W. E.; Fortt, S. Synthetic and Mechanistic Studies on the Antitumor Antibiotics Esperamicin-A1 and Calicheamicin-Gamma-1 - Synthesis of 2-Ketobicyclo[7.3.1] Enediyne and 13-Ketocyclo[7.3.1]

Enediyne Cores Mediated by Eta-2 Dicobalt Hexacarbonyl Alkyne Complexes - Cycloaromatization Rate Studies. *J. Am. Chem. Soc.* **1992**, *114*, 2544-2559.

47. Geivandov, R. K.; Kovshev, E. I. New Synthesis of 1,4-Dihydroxybicyclo[2.2.2]octane. *Zh. Org. Khim.* **1979**, *15*, 218-219.

48. Stemp, G.; Johnson, C. N. Bicyclic amine derivatives and their use as anti-psychotic agents. *WO9630333* **1996**.

49. Sasse, B. C.; Mach, U. R.; Leppaenen, J.; Calmels, T.; Stark, H. Hybrid approach for the design of highly affine and selective dopamine D-3 receptor ligands using privileged scaffolds of biogenic amine GPCR ligands. *Bioorg. Med. Chem.* **2007**, *15*, 7258-7273.

50. Stark, H.; Leppanen, J. M.; Sasse, B. C.; Saur, O.; Kottke, T.; Hill, M. P. Medicaments. *WO2009/056805A1* **2009**.

51. Tschammer, N.; Elsner, J.; Goetz, A.; Ehrlich, K.; Schuster, S.; Ruberg, M.; Kuhhorn, J.; Thompson, D.; Whistler, J.; Hubner, H.; Gmeiner, P. Highly Potent 5-Aminotetrahydropyrazolopyridines: Enantioselective Dopamine D-3 Receptor Binding, Functional Selectivity, and Analysis of Receptor-Ligand Interactions. *J. Med. Chem.* **2011**, *54*, 2477-2491.

52. Hayes, G.; Biden, T. J.; Selbie, L. A.; Shine, J. Structural subtypes of the dopamine D2 receptor are functionally distinct: expression of the cloned D2A and D2B subtypes in a heterologous cell line. *Mol. Endocrinol.* **1992**, *6*, 920-926.

53. Sokoloff, P.; Giros, B.; Martres, M. P.; Bouthenet, M. L.; Schwartz, J. C. Molecular cloning and characterization of a novel dopamine receptor (D3) as a target for neuroleptics. *Nature* **1990**, *347*, 146-151.

54. Asghari, V.; Sanyal, S.; Buchwaldt, S.; Paterson, A.; Jovanovic, V.; Van Tol, H. H. Modulation of intracellular cyclic AMP levels by different human dopamine D4 receptor variants. *J. Neurochem.* **1995**, *65*, 1157-1165.

55. Bettinetti, L.; Schlotter, K.; Hubner, H.; Gmeiner, P. Interactive SAR studies: rational discovery of super-potent and highly selective dopamine D3 receptor antagonists and partial agonists. *J. Med. Chem.* **2002**, *45*, 4594-4597.

56. Lowry, O. H.; Rosebrough, N. J.; Farr, A. L.; Randall, R. J. Protein measurement with the folin phenol reagent. *J. Biol. Chem.* **1951**, *193*, 265-275.

57. Cheng, Y.; Prusoff, W. H. Relationship between Inhibition Constant (Ki) and Concentration of Inhibitor Which Causes 50 Per Cent Inhibition (IC50) of an Enzymatic Reaction. *Biochem. Pharmacol.* **1973**, *22*, 3099-3108.

58. Bairoch, A.; Apweiler, R. The SWISS-PROT protein sequence database and its supplement TrEMBL in 2000. *Nucleic Acids Res.* **2000**, *28*, 45-48.

59. Larkin, M. A.; Blackshields, G.; Brown, N. P.; Chenna, R.; McGettigan, P. A.; McWilliam, H.; Valentin, F.; Wallace, I. M.; Wilm, A.; Lopez, R.; Thompson, J. D.; Gibson, T. J.; Higgins, D. G. Clustal W and Clustal X version 2.0. *Bioinformatics* **2007**, *23*, 2947-2948.

60. Hall, T. A. BioEdit: a user-friendly biological sequence alignment editor and analysis program for Windows 95/98/NT. *Nucleic Acids Symp. Ser.* **1999**, *41*, 95-98.

61. Sali, A.; Blundell, T. L. Comparative protein modelling by satisfaction of spatial restraints. *J. Mol. Biol.* **1993**, *234*, 779-815.

62. Frisch, M. J.; Trucks, G. W.; Schlegel, H. B.; Scuseria, G. E.; Robb, M. A.; Cheeseman, J. R.; Scalmani, G.; Barone, V.; Mennucci, B.; Petersson, G. A.; Nakatsuji, H.; Caricato, M.; Li, X.; Hratchian, H. P.; Izmaylov, A. F.; Bloino, J.; Zheng, G.; Sonnenberg, J. L.; Hada, M.; Ehara,

M.; Toyota, K.; Fukuda, R.; Hasegawa, J.; Ishida, M.; Nakajima, T.; Honda, Y.; Kitao, O.; Nakai, H.; Vreven, T.; Montgomery, J. A.; Peralta, J. E.; Ogliaro, F.; Bearpark, M.; Heyd, J. J.; Brothers, E.; Kudin, K. N.; Staroverov, V. N.; Kobayashi, R.; Normand, J.; Raghavachari, K.; Rendell, A.; Burant, J. C.; Iyengar, S. S.; Tomasi, J.; Cossi, M.; Rega, N.; Millam, J. M.; Klene, M.; Knox, J. E.; Cross, J. B.; Bakken, V.; Adamo, C.; Jaramillo, J.; Gomperts, R.; Stratmann, R. E.; Yazyev, O.; Austin, A. J.; Cammi, R.; Pomelli, C.; Ochterski, J. W.; Martin, R. L.; Morokuma, K.; Zakrzewski, V. G.; Voth, G. A.; Salvador, P.; Dannenberg, J. J.; Dapprich, S.; Daniels, A. D.; Farkas; Foresman, J. B.; Ortiz, J. V.; Cioslowski, J.; Fox, D. J. Gaussian 09, Revision B.01. In Wallingford CT, 2009.

63. Trott, O.; Olson, A. J. AutoDock Vina: improving the speed and accuracy of docking with a new scoring function, efficient optimization, and multithreading. *J. Comput. Chem.* **2010**, *31*, 455-461.

64. D.A. Case, T. A. D., T.E. Cheatham, III, C.L. Simmerling, J. Wang, R.E. Duke, R. Luo, M. Crowley, R.C. Walker, W. Zhang, K.M. Merz, B. Wang, S. Hayik, A. Roitberg, G. Seabra, I. Kolossváry, K.F. Wong, F. Paesani, J. Vanicek, X. Wu, S.R. Brozell, T. Steinbrecher, H. Gohlke, L. Yang, C. Tan, J. Mongan, V. Hornak, G. Cui, D.H. Mathews, M.G. Seetin, C. Sagui, V. Babin, and P.A. Kollman. AMBER 10. **2008**.

65. Hornak, V.; Abel, R.; Okur, A.; Strockbine, B.; Roitberg, A.; Simmerling, C. Comparison of multiple Amber force fields and development of improved protein backbone parameters. *Proteins* **2006**, *65*, 712-725.

66. Wang, J.; Wolf, R. M.; Caldwell, J. W.; Kollman, P. A.; Case, D. A. Development and testing of a general amber force field. *J. Comput. Chem.* **2004**, *25*, 1157-1174.

67. Bayly, C. I.; Cieplak, P.; Cornell, W.; Kollman, P. A. A well-behaved electrostatic potential based method using charge restraints for deriving atomic charges: the RESP model. *J. Phys. Chem.* **1993**, *97*, 10269-10280.

Table of Contents Graphic